TÉCNICO LISBOA

Small-Cell LTE Networks: Evaluating RF Planning Methods

Inês Moura Perdigão Gonçalves

Thesis to obtain the Master of Science Degree in

Electrical and Computer Engineering

Supervisor(s): Prof. António José Castelo Branco Rodrigues
Prof. Maria Paula Dos Santos Queluz Rodrigues

Examination Committee

Chairperson: Prof. José Eduardo Charters Ribeiro da Cunha Sanguino
Supervisor: Prof. António José Castelo Branco Rodrigues
Member of the Committee: Prof. Pedro Manuel de Almeida Carvalho Vieira

November 2018

Declaration

I declare that this document is an original work of my own authorship and that it fulfills all the requirements of the Code of Conduct and Good Practices of the Universidade de Lisboa.

Dedicated to my family.

Acknowledgments

First of all, I would like to thank my supervisor Prof. António Rodrigues and co-supervisor Prof. Paula Queluz Rodrigues for the opportunity to work on this thesis and the guidance and support shown during this last year. I would also like to thank Instituto de Telecomunicações for providing me with the required means for the completion of this dissertation.

I would like to express my gratitude to Nuno Marques and Nokia Portugal for the incredible opportunity given to develop my master thesis in a business environment.

A special thanks to Tiago Gonçalves without whom this thesis could not have happened. His continuous guidance, as well as knowledge and suggestions were essential. In addition, to all my colleagues at Nokia for all the encouragement and advices I received.

I would also like to thank my parents and sister for all their encouragement and unconditional support not only during the development of this thesis but essentially throughout my life.

A special thanks to all my friends but especially to the ones I have made in Técnico and that made it even more worthwhile: Inês, João, Maria, Rita and Vera. A very special thanks to Miguel for everything, including for even trying to read this thesis.

Abstract

This work focuses on the study and evaluation of different propagation models and geographical databases used in the planning of LTE networks. A key aspect of the study includes the comparison of the distinct types of databases used: 2D, 2.5D and 3D.

Two separate studies were performed: a coverage by area and a point-to-point. The coverage by area analysis used a buffer area, which recreated the path followed in the walk test, to simulate the RSRP and RSRQ levels obtained with each model. The point-to-point study used the location of the walk test samples to obtain the equivalent predicted values. The models simulated are Okumura-Hata, COST 231-Hata, SPM and WinProp UDP.

A detailed analysis of the simulations and their comparison to the results obtained during the walk test led to several conclusions. Although the Okumura-Hata model obtained the lowest mean absolute error, it was the WinProp UDP Outdoor model that overall showed the best performance regardless of the analysis method. SPM 2D was the model that adapted better when the walk test samples had a RSRP level higher than -85 dBm, while COST 231-Hata obtained the best results in the opposite scenario. A relevant conclusion stresses the importance of accurate drive tests and their validity, as well as the clear improvement obtained in network planning when using dominant path models.

Keywords: LTE, propagation models, walk test, clutter classes

Resumo

Este trabalho baseia-se no estudo e avaliação de diferentes modelos de propagação e bases de dados geográficas utilizados no planeamento de redes LTE. Um aspecto essencial deste estudo inclui a comparação dos distintos tipos de bases de dados utilizadas: 2D, 2.5D e 3D.

Foram efetuados dois estudos em paralelo: o de cobertura por área e o de ponto-a-ponto. A análise da cobertura por área utilizou a área de um *buffer*, que recriava o caminho percorrido no *walk test* de forma a simular os níveis de RSRP e RSRQ obtidos por cada modelo. O estudo ponto-a-ponto utilizou a posição de cada amostra do *walk test* para obter os valores simulados. Os modelos simulados foram: Okumura-Hata, COST 231-Hata, SPM e WinProp UDP.

Uma análise detalhada das simulações e a sua comparação com os resultados obtidos durante o *walk test* levou a várias conclusões. O modelo Okumura-Hata obteve o menor erro absoluto médio mas o WinProp UDP Outdoor foi o modelo que mostrou uma melhor desempenho independentemente do método de análise. Ao avaliar os modelos de acordo com o alcance, verificou-se que o SPM 2D foi o que melhor se adaptou quando as amostras do *walk test* tinham valores superiores a -85 dBm, enquanto o COST 231-Hata obteve os melhores resultados no cenário oposto. Como conclusão relevante destaca-se a importância da precisão dos *drive tests* e da sua validade, assim como a melhoria considerável que os modelos de caminho dominante trazem ao planeamento de redes.

Palavras-chave: LTE, modelos de propagação, *walk test*, classes de *clutter*

Contents

List of Figures

List of Tables

Acronyms

2G 2nd Generation

3G 3rd Generation

3GPP 3rd Generation Partnership Project

4G 4th Generation

ABS Almost Blank Subframes

AMC Adaptive Modulation and Coding

AP Access Point

CB Coordinated Beamforming

CINR Carrier to Interference-and-Noise Ratio

CoMP Coordinated Multipoint

CP Cyclic Prefix

CS Coordinated Scheduling

CSG Closed Subscriber Group

DL Downlink

DPM Dominant Path Model

DSL Digital Subscriber Line

DTM Digital Terrain Model

E-UTRAN Evolved Universal Terrestrial Radio Access Network

eICIC Enhanced ICIC

EIRP Effective Isotropic Radiated Power

eNB evolved NodeB

EPC Evolved Packet Core

EPS Evolved Packet System

FDD Frequency Division Duplexing

FFR Fractional Frequency Reuse

GPS Global Positioning System

GSM Global System for Mobile Communications

HeMS HeNB Management System

HeNB Home eNB

HeNB-GW Home eNB Gateway

HetNet Heterogeneous Network

HSS Home Subscriber Server

ICIC Inter-Cell Interference Coordination

IDP Indoor Dominant Path

IP Internet Protocol

IPsec Internet Protocol Security

IRT Intelligent Ray Tracing

ISI Inter-Symbol Interference

ITU-R Radio Communication Sector of the International Telecommunication Union

JP Joint Processing

LOS Line of Sight

LTE Long Term Evolution

LTE-A LTE Advanced

MIMO Multiple Input Multiple Output

MISO Multiple Input Single Output

MLPD Minimum Loss Dominant Path

MME Mobility Management Entity

NLOS Non Line of Sight

OFDM Orthogonal Frequency Division Multiplexing

OFDMA Orthogonal Frequency Division Multiple Access

P-GW PDN Gateway

PAR Peak-to-Average Ratio

PCRF Policy Control and Charging Rules Function

PDN Packet Data Network

QAM Quadrature Amplitude Modulation

QoS Quality of Service

QPSK Quadrature Phase Shift Keying

RAT Radio Access Technologies

RB Resource Block

RE Resource Element

RSRP Reference Signal Received Power

RSRQ Reference Signal Received Quality

RSSI Receive Signal Strength Indicator

S-GW Serving Gateway

S1-U S1 User Plane

SAE System Architecture Evolution

SC-FDMA Single Carrier Frequency Division Multiple Access

SeGW Security Gateway

SIMO Single Input Multiple Output

SINR Signal-to-Interference-plus-Noise Ratio

SNR Signal-Noise Ratio

SPM Standard Propagation Model

TDD Time Division Duplexing

TDM Time Division Multiplexing

TTT Time To Trigger

UDP Urban Dominant Path

UE User Equipment

UL Uplink

UMTS Universal Mobile Telecommunications System

UTRAN Universal Terrestrial Radio Access Network

Wi-Fi Wireless Fidelity

Chapter 1

Introduction

This chapter introduces the theme of this thesis, situating the matter in a global scale. The motivation and structure of the thesis are also presented.

1.1 Overview

Over the last decades, fuelled by our need to communicate and the technological advances, there has been a dramatic change in the way we communicate that in time altered consumer's needs. In the beginning of digital cellular networks the technologies developed, like the Global System for Mobile Communications (GSM), were designed to primarily focus on voice traffic. Only later on, the data capabilities were added. Although data use increased throughout the years, most of the traffic volume in 2nd Generation (2G) networks was still voice traffic. The global availability of user-friendly mobile communications combined with increasing consumer familiarity and practical reliance on those technologies, provided the context for new systems with advanced capabilities. [1]

The introduction of 3rd Generation (3G) networks, such as the Universal Mobile Telecommunications System (UMTS), instigated an increased usage of data by enabling various new services like the Global Positioning System (GPS), mobile television and video conferencing.

The Long Term Evolution (LTE), commonly known as 4th Generation (4G), is the first cellular communication system designed specifically to support packet-switched data services since the beginning. It provides higher data rates than previous mobile systems, combined with wide-area coverage and seamless support for mobility, including between different radio-access technologies. According to its requirements LTE should provide peak user throughput with a minimum of 100 Mbit/s in the Downlink (DL) and 50 Mbit/s in the Uplink (UL). It was also defined that there should be reduced delays, in terms of connection establishment and transmission latency. Another requirement was the need for greater flexibility of spectrum usage, in both new and pre-existing bands.

Nowadays, trends have shown an immeasurable growth of data traffic that clearly dominates in comparison to voice traffic. Mobile data traffic has grown 18-fold between 2011 and 2016 and global mobile data traffic grew 63% in 2016. Although 4G connections represented only 26% of mobile connections

in 2016, they already accounted for 69% of mobile data traffic, while 3G connections represented 33% of mobile connections and 24% of the traffic, as pictured in Figure 1.1. According to predictions from [2], global mobile data traffic will increase 7-fold between 2016 and 2021 and is expected to reach 49 exabytes per month. By 2021, 4G will correspond to 53% of all connections and 79% of the total traffic.

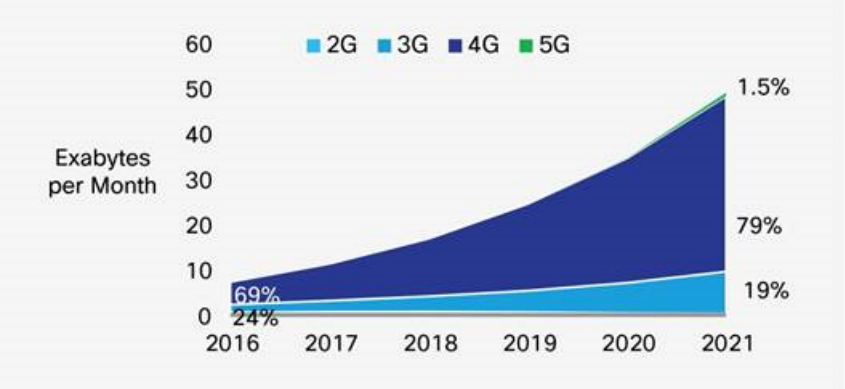

Figure 1.1: Global Mobile Traffic by Connection Type (extracted from [2]).

From a regional point of view, Asia Pacific will account for 47% of global mobile traffic by 2021, the largest share of traffic by a substantial margin, as shown in Figure 1.2. North America, which had the second-largest traffic share in 2016, will have only the fourth-largest share by 2021, having been surpassed by Central and Eastern Europe and Middle East and Africa.

Figure 1.2: Global Mobile Data Traffic Forecast by Region (extracted from [2]).

1.2 Motivation and Contents

As the capacity demand in mobile networks increased, the development of new wireless communication technologies that solved some of the existing constraints related to radio spectral resources became crucial. Small-cells were presented as a promising solution to increase the capacity and coverage of the network by offloading the macro layer and increasing Quality of Service (QoS). These low power base stations can be deployed both with macro coverage and standalone, both indoor and outdoor. However, the location of the deployment of small-cells demands some planning as it can cause interference with macro cells in the area.

One of the tools that contributes to an efficient planning is the use of the correct propagation model for the area in question and the fine-tuning performed afterwards. The increased complexity of mobile networks in urban areas has made the propagation models and the geographical databases used essential. The main scope of this thesis is to analyse different propagation models used in the planning and deployment of small-cells in a typical urban scenario.

The objective is to compare real data obtained in a walk test with predictions of different propagation models and geographical databases in a LTE network using a radio network planning software. This thesis was developed in collaboration with Nokia Portugal. This partnership was essential, as it allowed for a realistic study using data obtained in an actual project.

This thesis is divided in 5 chapters, including the present one. Chapter 2 introduces LTE and reviews some of its basic features. The overall network architecture is described, followed by the main features of the radio interface. In the same chapter, small-cells are also introduced and discussed. The following section introduces the distinct propagation models. Lastly, the state of the art reviews some of the existing literature related to the scope of this thesis.

In Chapter 3, the methodology followed in this thesis is presented. First, some context is given to explain the origin of the work here presented. Then, the propagation models used in each of the predictions are more thoroughly described. A following section illustrates some of the adjustments and corrections that were performed to the data obtained in the walk test to reduce possible inconsistencies found between measured and predicted results. An assessment of each of the models is provided in the final section of chapter 3, so that it is ensured that the results given by the simulations are relevant.

The analysis of the results is presented in Chapter 4. The results obtained through measurements during the walk test are analysed and also compared to the simulations results. Two separate and major analysis are performed according to each propagation model: the coverage by area and the point-to-point coverage.

Chapter 5 contains a general analysis of the obtained results and the main conclusions of this thesis, followed by suggestions for future work. A summary of all the work performed is also provided, so that one can have a general understanding of the thesis and the conclusions obtained in the end.

Chapter 2

Fundamental Concepts

This chapter provides an overview of the basic concepts of LTE, such as the network architecture and the radio interface. It also presents small-cells and discusses some of its main features like network architecture, interference and mobility. Then, the different types of propagation models and geographical databases are introduced. Furthermore, a brief state of the art is provided in the final section.

2.1 LTE

LTE is a wireless communication standard developed by the 3rd Generation Partnership Project (3GPP), aimed at enhancing the Universal Terrestrial Radio Access Network (UTRAN) and optimizing the radio access architecture. Although LTE is commonly referred to as 4G, initially it did not meet the technical requirements of a 4G wireless service set by the Radio Communication Sector of the International Telecommunication Union (ITU-R). However, due to the significant advancements it brought with regards to the 3G technologies, it was later accepted as 4G. The LTE Advanced (LTE-A) standard, a major enhancement of LTE, satisfies the original requirements of the ITU-R and has been labelled as ”True 4G”.

Some of the driving forces for the development of LTE include the increased capability of existing wireline technologies, the need for additional wireless capacity, as well as the need for lower cost wireless data delivery and the existing competition with other wireless technologies. The main requirements for this standard included high spectral efficiency, high peak data rates, short round trip time as well as flexibility in frequency and bandwidth.

2.1.1 Network Architecture

This section is based on [1] and [3].

LTE was designed to support only packet-switched services in contrast to the circuit-switched data services of the previous generations. Its objective is to provide continuous Internet Protocol (IP) connectivity between the User Equipment (UE) and the Packet Data Network (PDN) without disruptions during mobility.

The “evolution” stated in LTE, refers not only to the evolution of the radio access network, now named Evolved Universal Terrestrial Radio Access Network (E-UTRAN), but also to the evolution of the non-radio aspects. This results in the System Architecture Evolution (SAE) which includes the Evolved Packet Core (EPC) network. The Evolved Packet System (EPS), represented in Figure 2.1, corresponds to the set of both LTE and SAE.

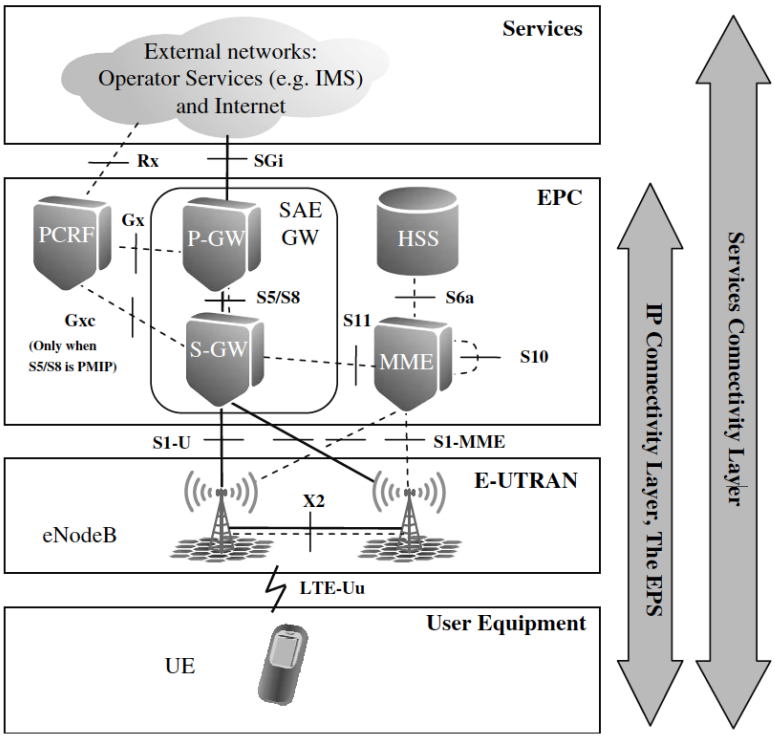

Figure 2.1: EPS Architecture (extracted from [3]).

The E-UTRAN connects the UE to the EPC and is simply composed by one type of node — evolved NodeB (eNB). These eNBs can cover one or more cells and are capable of handling all the radio related protocols. As such, LTE networks are said to be flat because there is no centralized controller. This allows to speed up the connection set-up and reduce the time required for a handover. The eNBs are inter-connected via the X2-interface and connected to the EPC by the S1-interface, as illustrated in Figure 2.2. These interfaces are standardized in order to allow multi vendor interoperability.

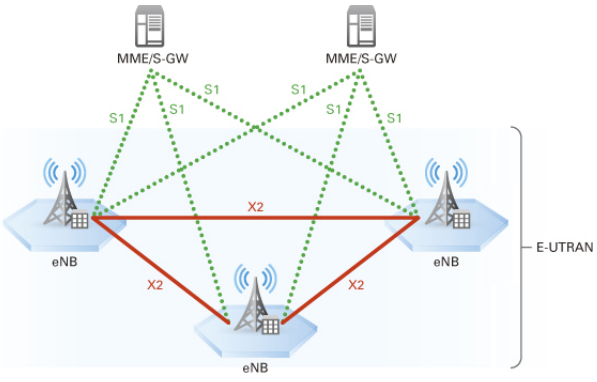

Figure 2.2: E-UTRAN Architecture (extracted from [4]).

The E-UTRAN is responsible for all the radio related functions which includes the management of radio resources, header compression, security and connectivity to the EPC. The radio resource management includes tasks such as the allocation of resources based on requests, prioritizing and scheduling traffic according to QoS parameters and continuous overseeing of the resources consumption.

The main logical nodes of the EPC, as seen in Figure 2.3, are the Serving Gateway (S-GW), the PDN Gateway (P-GW) and the Mobility Management Entity (MME). Other logical nodes include the Home Subscriber Server (HSS) and the Policy Control and Charging Rules Function (PCRF).

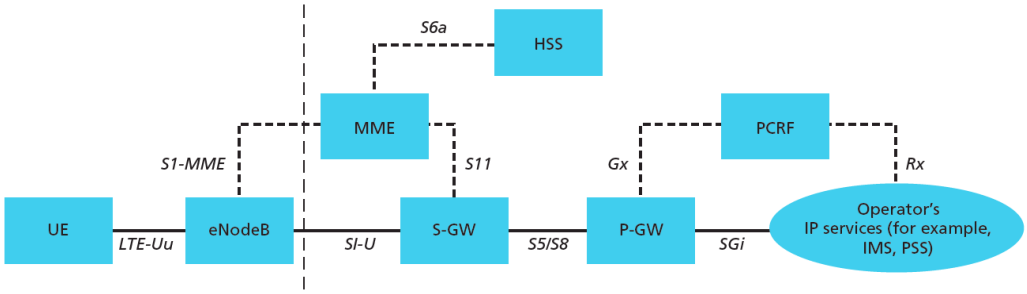

Figure 2.3: EPS Network Elements (extracted from [5]).

The S-GW serves as mobility anchor for interworking with other 3GPP technologies and as a local mobility anchor for the data bearers when the UE moves between eNBs. A bearer is an IP packet flow with a defined QoS between the gateway and the UE. The transfer of all user IP packets is done by this node. The P-GW is the highest level mobility anchor in the system. When a UE moves from one S-GW to another, its bearers must be switched in the P-GW. This node typically allocates IP addresses for the UE and enforces QoS and flow-based charging. It also serves as mobility anchor for interworking with other non-3GPP technologies.

The MME is the main control element in the EPC and handles the control plane signalling. It is also responsible for the management of connectivity services and subscription profiles, authentication procedures and security. The HSS corresponds to the main database regarding all permanent subscription data, such as the subscribed QoS profile, any access restrictions for roaming and information about the PDNs to which the user can connect. The PCRF is in charge of policy control decision-making. It also manages the QoS authorizations and ensures it is in accordance with the users subscription.

2.1.2 Radio Interface

This section presents an overview of the radio interface of LTE based on [3], [6] and [7].

LTE operates in different arrangements of frequency and bandwidth, depending on the region where it is implemented. The range of channel bandwidth varies from 1.4 MHz to 20 MHz. ANACOM, the Portuguese Telecommunications Authority, subsequently to the auction for allocation of rights of use of frequencies determined the bands around 800 MHz, 900 MHz, 1800 MHz and 2600 MHz for LTE. [8]

As LTE had higher requirements, an improved use of the spectrum was necessary. Another relevant aspect which had to be accounted for was the need for flexibility regarding users with different needs

relating to network usage. Consequently, selecting a suitable modulation scheme and multiple access technique is essential in order to accomplish such targets.

In LTE, the multiple access is based on the Orthogonal Frequency Division Multiple Access (OFDMA) for the DL and on the Single Carrier Frequency Division Multiple Access (SC-FDMA) for the UL, both with Cyclic Prefix (CP). The CP is added by copying part of the symbol at the end and attaching it to the beginning of the symbol. The signal will gain a periodic nature, allowing discrete Fourier operations, hence avoiding Inter-Symbol Interference (ISI). There are two sets of CP based on their duration: the extended CP and the short CP corresponding to seven and six Orthogonal Frequency Division Multiplexing (OFDM) symbols per slot, respectively. The length that characterizes the CP plays an important role: if it is too short, it becomes impossible to avoid the multi-path reflection delay spread, but if it is too long, it narrows the data throughput capacity.

The transmission in OFDMA is based on the use of narrow, mutually orthogonal sub-carriers. In LTE, each sub-carrier is spaced 15 kHz regardless of the total transmission bandwidth. At the sampling instant of a single sub-carrier, all the others have zero value, as shown in Figure 2.4. The orthogonality achieved by the sub-carrier allows for a more efficient use of the spectrum, because a band guard is no longer needed to avoid sub-carrier interference. The elimination of the band guard increases the simultaneous transmission of symbols, increasing the overall transmission rate.

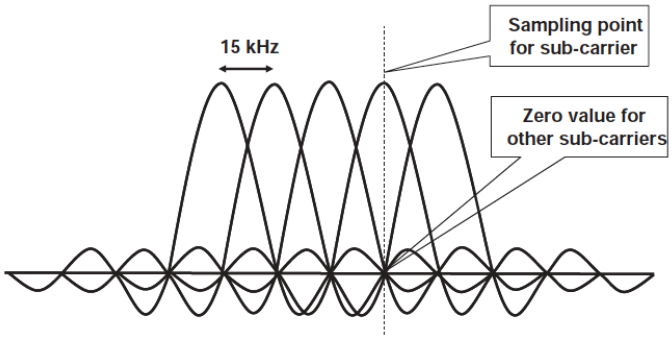

Figure 2.4: Mutually Orthogonal Sub-Carriers (extracted from [6]).

The data to be transmitted by the user is divided in multiple data sub-fluxes, modulated into different OFDMA sub-carriers, which will simultaneously be transmitted, generating a high speed data flow. One of the main challenges in OFDMA is the high Peak-to-Average Ratio (PAR) of the transmitted signal. This not only limits the transmitted power and reduces coverage but forces the use of better power amplifiers. The UL signal is generated by the users' mobile terminal so in this scenario a multiple access technique that enables better power-amplifier efficiency is needed. This was solved by choosing the SC-FDMA in the UL.

Similarly to OFDMA, SC-FDMA divides the transmission bandwidth into multiple parallel subcarriers maintaining the orthogonality of the subcarriers. However, in SC-FDMA the data symbols are not directly assigned to each subcarrier independently like in OFDMA. Instead, the signal which is assigned to each subcarrier is a linear combination of all modulated data symbols transmitted at the same time instant. [9]

Regarding the use of OFDMA, it must be noted that a base station transmitter can allocate its users to basically any sub-carrier in the frequency domain. By having different sub-carriers allocated to users, the scheduler benefits from frequency diversity. But the allocation is not done on an individual sub-carrier level basis due to overhead caused by signalling. Instead the allocation is based on Resource Blocks (RBs) each consisting of 12 sub-carriers, thus resulting in 180 kHz. In the time domain, a RB corresponds to a 0.5 ms slot and 2 slots correspond to a sub-frame with a 1 ms duration. Finally, a frame is a group of 10 sub-frames. The smallest unit corresponds to the Resource Element (RE), which consists of one sub-carrier with the duration of one OFDM symbol. As the range of bandwidth varies from 1.4 MHz to 20 MHz and each RB corresponds to 180 kHz that will correspond to 6 RBs and 100 RBs, respectively. The DL physical resource can be represented as a time-frequency resource grid, as depicted in Figure 2.5.

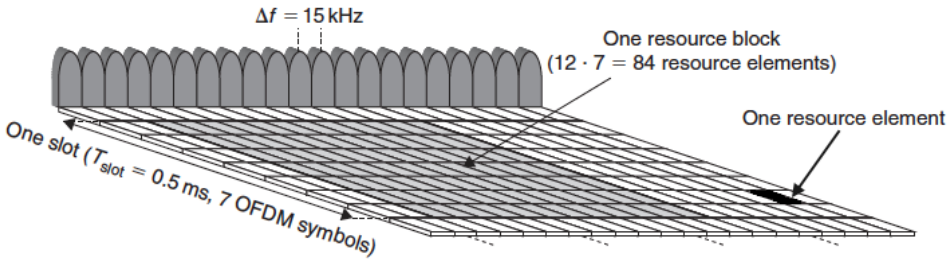

Figure 2.5: Downlink Physical Resource (adapted from [7]).

A high degree of spectrum flexibility is one of the main characteristics of the LTE radio access. LTE supports two types of duplexing: Time Division Duplexing (TDD) and Frequency Division Duplexing (FDD) although FDD is the most adopted technique. In TDD, the DL and UL use the same frequency but transmission takes place in different, non-overlapping time slots. Contrarily, FDD implies that DL and UL transmissions take place in different, sufficiently separated, frequency bands but simultaneously.

Mobility management plays a vital part in any wireless telecommunications system. LTE aims to provide seamless mobility while maintaining a low network complexity. The UE state for the mobility support in LTE systems according to 3GPP is classified in two states: idle mode and connected mode. When a UE is in idle mode it is switched on but it has no active connection (bearer) to the network. On the other hand, when a UE is in connected mode it is transmitting data to the network. The mobility in idle mode is performed autonomously by the UE based on its own measurements. In connected mode, the mobility management is performed by the UE that sends measurement reports to the E-UTRAN which will decide whether or not to trigger a handover to another base station. The 3GPP specifies the handover procedure that supports the users' mobility, as such the handovers in LTE are hard handovers. In other words, there is a short interruption in service when the handover is performed. In a soft handover the UE is always connected to at least an eNB. While soft handovers can almost always maintain the service connection, they require more signalling and protocol. Therefore, low-complexity hard handovers are used in LTE networks at the risk of service disruption. [10]

The handover process is divided into four parts, as shown in Figure 2.6. The procedure starts with

the UE measuring the signal of the neighbour cell, as represented by (1). Afterwards, the measurement results are processed in the UE, as represented by (2). When the neighbours' cell Reference Signal Received Power (RSRP) exceeds the serving cells' RSRP by a specific amount during at least the Time To Trigger (TTT), the UE will send a measurement report to the serving cell to request handover (3). The handover decision is made at the serving cell based on the received measurement reports, as denoted by (4).

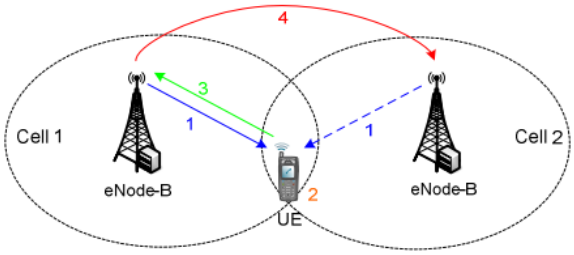

Figure 2.6: Handover Process in Macro Cells (adapted from [11]).

2.1.3 Modulation

LTE uses 3 types of Quadrature Amplitude Modulation (QAM). They are the Quadrature Phase Shift Keying (QPSK) or 4-QAM, 16-QAM and 64-QAM modulation schemes. The 256-QAM was added in Release 12, which corresponds to the release of LTE-A. The QPSK carries 2 bits per symbol while 16-QAM and 64-QAM carry 4 and 6 bits per modulation symbol, respectively. These modulation schemes are available in both UL and DL directions in all devices, except for 64-QAM in the UL which depends on the UE capability. The QPSK is the most robust to interference and bad channel conditions, but consequently offers the lower bit rate. In contrast, the 64-QAM allows the higher bit rates in LTE, but requires the best conditions in terms of Signal-to-Interference-plus-Noise Ratio (SINR), by being the most liable to errors due to interference.

A technique developed to improve system capacity and also coverage reliability that had already been used in several other 3GPP systems, named Adaptive Modulation and Coding (AMC) was proposed for LTE. In order to make better use of channel capacities and improve efficiency, the AMC matches coding rates and modulation schemes to the radio channel conditions. For any given modulation scheme, the appropriate code rate can be chosen, depending on channel quality of each user. In order to maximize system throughput and to achieve the maximum channel quality, higher order modulation schemes and higher code rates can be selected if the channel conditions allow it. With this capability of self-optimization comes an overall improved system.

2.1.4 MIMO

LTE was the first global mobile system to be designed with Multiple Input Multiple Output (MIMO) as a key component from the very beginning. This technology relies on using multiple antennas in the transmitter and receiver ends in order to take advantage of spatial, pre-coding and transmit diversity.

Depending on the availability of multiple antennas at the transmitter and/or the receiver, such techniques are classified as Single Input Multiple Output (SIMO), Multiple Input Single Output (MISO) or MIMO, as presented in Figure 2.7.

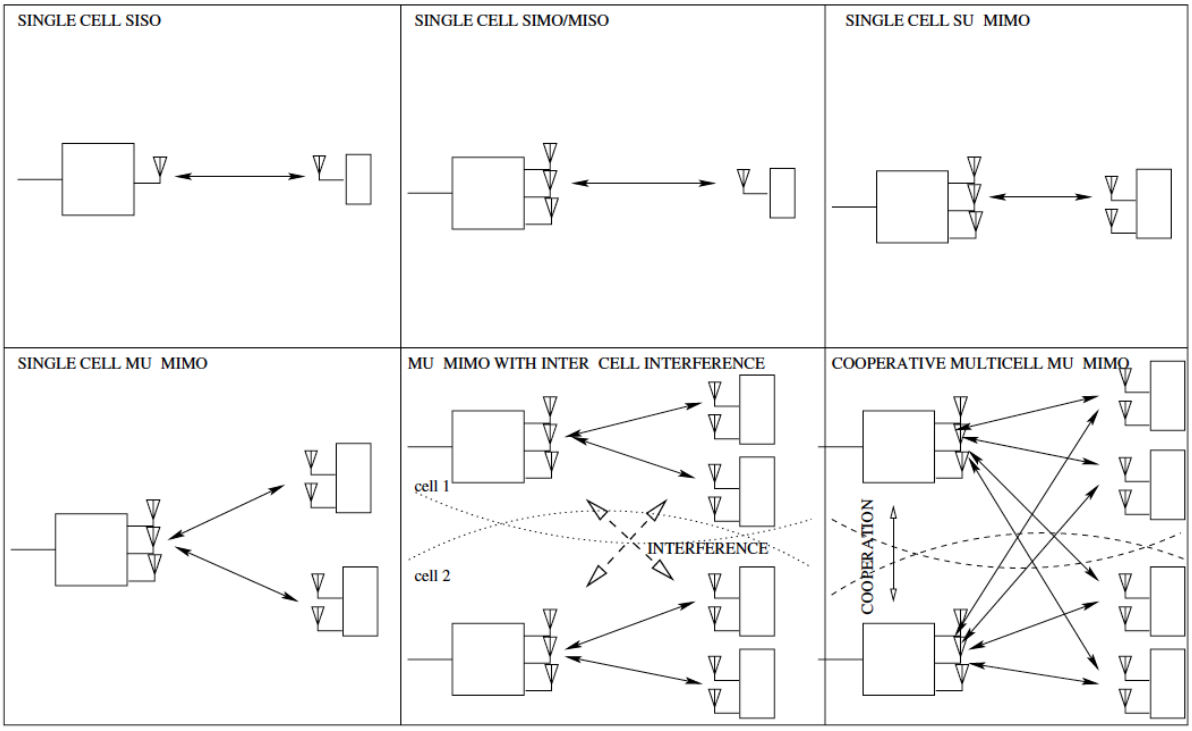

Figure 2.7: Different Usages of the MIMO Technology (extracted from [1]).

Spatial multiplexing consists in the signal transmission from two or more different antennas with different data streams, with later separation through signal processing in the receiver. Thus, with a 2-by-2 antenna configuration the peak data rates can be doubled. If applied with a 4-by-4 antenna configuration the peak data rates can increase fourfold. Pre-coding is fundamentally related to the weighting of the signals transmitted from different antennas, in order to maximize the received Signal-Noise Ratio (SNR). Lastly, transmit diversity consists in the transmission of the same signal from different antennas using some coding to exploit the gains from independent fading between the different antennas.

2.2 Small-Cells

The unmeasured usage growth of cellphones, tablets and data-hungry applications has caused an exponential growth of traffic in mobile networks, as stated before. Operators have met this challenge by increasing capacity with new radio spectrum, adding multi-antenna techniques and implementing more efficient modulation and coding schemes. However, these measures alone are insufficient in extremely crowded environments and at cell edges where performance can significantly degrade. Complementing macro networks with small-cells is an effective way to extend coverage and increase capacity indoors and outdoors, in public spaces, offices or residences.

2.2.1 Types of Small-Cells

This section is based on [12].

Small-cells are operator-controlled, low-powered radio access nodes, used to complement mobile services that is served by macro cells. They are primarily deployed to increase capacity in hot spots with high user demand and to fill in areas not covered by the macro network both outdoors and indoors. Small-cells also improve network performance and service quality by offloading from the large macro cells. A combination of macro cells and small-cells is usually called as a Heterogeneous Network (HetNet) that provides increased bitrates per unit area.

There are different types of small-cells which can be grouped according to cell size: femtocells, picocells and microcells, as represented in Figure 2.8.

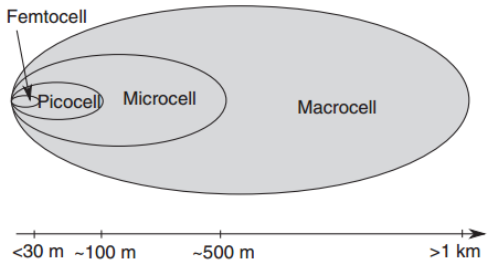

Figure 2.8: Cell Sizes of Different Technologies (extracted from [12]).

These range from very compact residential femtocells to larger equipment used inside commercial offices or even in outdoor public spaces. These various types of small-cells are developed as an attempt to respond to different consumers' needs when it became obvious that macro cells were not enough.

Operators began to install smaller outdoor base stations called microcells as new data services that required higher coverage, emerged. These are deployed in specific areas in which extra capacity is known to be needed, for example near a train station or in a city centre. They are also often temporarily deployed during special occasions like sporting events. Adding microcells in the urban environment allows the operator to subdivide the cells, leading to an optimization of the use of the spectrum and ensuring a better capacity. Microcells have a range of a few hundred metres.

Both macro cells and microcells only indirectly optimise the indoor coverage by increasing the outdoor coverage. The need to optimise specifically the indoor coverage led to the development of technologies like the picocells and femtocells.

Picocells are small base stations that work very similarly to an Access Point (AP). An AP is a device that by using an integrated antenna enables a connection between the user and the Internet. These are used to access broadband Internet connection via air interface in the Wireless Fidelity (Wi-Fi) technology. Picocells have a low power radiating antenna that connects to the operator's core network. It manages the transmission of data between the picocell and the network, performs the handover between the cells and allocates resources to different users. The picocell is connected to the core network via standard in-building wiring, fibre optic or Ethernet connection.

An optimal solution for the deployment of picocells would be one where the number of picocells is

sufficient to ensure the coverage and capacity requirements, while not creating interference. This phenomenon of interference with neighbouring outdoor cells is an additional consequence of using small-cells, but one that should be minimized. Therefore, combined indoor/outdoor network planning is a vital issue.

Picocells can be used in business environments, shopping centres and airports, for example. They are also useful in high-rise buildings, where the macro cell signal strength decreases with height. The main advantage is that they are considerably cheaper and since they are placed indoor, they effectively increase indoor radio coverage and capacity. Picocells have a range of approximately 100 metres.

Femtocells were proposed to extend the concept of picocells to home networks, in particular. They have limited output power, between 10 and 20 dBm, and capacity as they serve 4 to 6 users. These type of small-cells can be deployed in a variety of scenarios. A typical deployment is in a rural environment, where a femtocell enables access to mobile network for users which are typically under a coverage hole but with a reliable Digital Subscriber Line (DSL) connection. As it happens homes in rural areas usually lack the macro cell coverage, but some already have access to high data rate Internet, making it an ideal scenario to deploy femtocells.

Another use case case for femtocells is an enterprise environment, where the low capacity of femtocells is typically enough to cover a number of offices. Regarding the access mode of femtocells, this can be private or public. In an office environment, the femtocells would have to be deployed as public access so that any user can access them. But in a home environment these cells should be deployed in a private access mode. This means the subscriber of a femtocell will define the authorised list of users, so called Closed Subscriber Group (CSG) that has permission to access the femtocell.

The major advantage of femtocells is the fact they are directly installed by the end users inside their homes and have a maximum range of approximately 30 metres. This will ensure good coverage for subscribers. For operators, femtocells are a cheap solution because they are paid by customers.

2.2.2 Network Architecture

This section is based on [12] and [13].

With the deployment of femtocells the general network architecture suffered some changes. The Home eNB (HeNB) that incorporates the capabilities of a regular eNB was the major change introduced. In addition, the Home eNB Gateway (HeNB-GW), Security Gateway (SeGW) and HeNB Management System (HeMS) were are also added. According to the 3GPP, there are three possible architectures, that depend if the HeNB-GW is present or not and in the first case, whether the S1 User Plane (S1-U) goes through it or not. The basic E-UTRAN HeNB architecture is presented in Figure 2.9.

When the HeNB-GW is present in the network, it is placed between the HeNB and the MME and it aggregates traffic from a large number of HeNBs back into an existing core service network through the standard S1 interface. The HeNB-GW is installed within an operator's network. Some of the basic functions of the SeGw include securing the communication to and from the HeNBs. It authenticates the HeNBs and establishes Internet Protocol Security (IPsec) tunnels with HeNBs. IPsec tunnels are

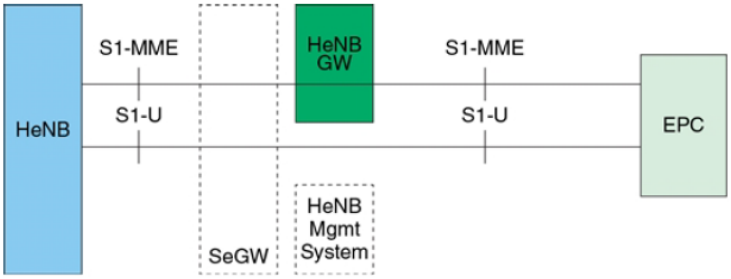

Figure 2.9: E-UTRAN HeNB Logical Architecture (extracted from [14]).

responsible for delivering all voice, messaging and packet data services between HeNB and the core network. The SeGW can be implemented as a separate physical entity or in an existing entity. The HeMS is used to ensure that the services provided to the user are of high quality and sufficiently secured. While managing the HeNB access network, the HeMS also facilitates the HeNB-GW discovery and provisions the configuration data to the HeNB.

The HeNBs are inter-connected via the X2-interface and connected to the EPC by the S1-interface. More specifically, the S1-U interface links the HeNB and the core network and the S1-MME interface establishes the connection between the HeNB and the HeNB-GW.

2.2.3 Interference

This section is based on [15], [16] and [17].

The use of small-cells introduced changes to the topology of conventional macro cellular networks. The new network is now composed by two distinct layers: the macro cell layer and the small-cell layer. The first layer relates to the plain old traditional cellular network while the second one includes several shorter range cells that can be planned (microcells) or distributed in a random manner (femtocells). The existence of these two layers creates new interference problems. To achieve the desired performance, interference management methods need to be employed.

Traditionally, inter-cell interference was limited to cell-edge areas, which were covered by more than one cell. With the deployment of small-cells, interference is increasingly originated from small-cell coverage areas located inside the macro cell coverage area. Another particular case is intra-cell interference. This relates to different UEs within the same coverage area, interfering with each other. Overall, two types of interference can occur: co-layer interference and cross-layer interference. The former of which if the interfering systems belong to the same layer and the latter if they belong to different layers. These different types of interference are depicted in Figure 2.10.

A number of solutions have been developed to mitigate the increasing interferences, such as Inter-Cell Interference Coordination (ICIC), Enhanced ICIC (eICIC) and Coordinated Multipoint (CoMP) transmission and reception.

The ICIC technique mitigates interference and improves performance by coordinating network resources across neighbouring cells. One of the static mechanisms managed by the ICIC is the Fractional Frequency Reuse (FFR). It divides each cell in inner and outer parts and allocates the spectrum accord-

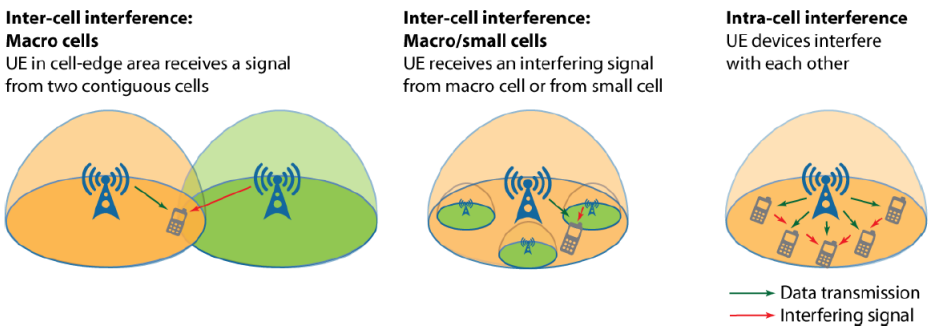

Figure 2.10: Different Types of Interference (extracted from [16]).

ingly. In the cell centre, the whole spectrum can be used for transmission. Users in the outer part of the cell will only be assigned part of the spectrum according to their orientation in the cell area. This approach is comparable to using a frequency reuse of 1 in the area immediately surrounding the cell site and a frequency reuse of 3 at the cell edge, as seen in Figure 2.11.

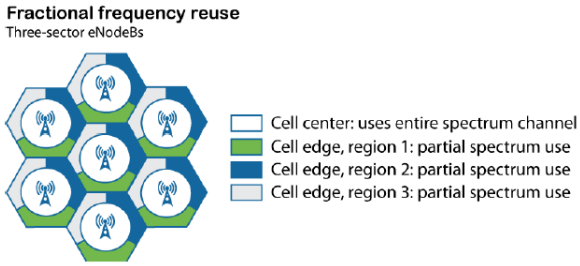

Figure 2.11: Fractional Frequency Reuse (extracted from [16]).

As the ICIC evolved to better support HetNet deployments the eICIC was created. This technique addresses cross-layer interference. The major change is the addition of the time domain through the use of Almost Blank Subframes (ABS) in a semi-static pattern. Each ABS includes only control channels and cell-specific reference signals, no user data. With the Time Division Multiplexing (TDM) eICIC, while one of the interfering cells sends an ABS, the other cell successfully sends a subframe that contains data. Tight coordination between the HeNB and the macro eNB is required, using the X2 interface since the sending of ABSs alternates between the two cells that interfere with each other.

One other technique used is CoMP. It includes various tools that minimize inter-cell interference when one or more UE devices are located at the cell edge and receive signals from more than one cell. The first main component in CoMP is Joint Processing (JP). JP allows to simultaneously transmit to a single UE device from multiple cells and also to receive the transmitted signal at multiple cells. Other mechanisms used include Coordinated Scheduling (CS) and Coordinated Beamforming (CB). CS uses the signalling between two cells to determine which one should transmit a subframe to the UE. Using CB, the transmitting beam is narrowly directed to the desired UE thus reducing interference.

2.2.4 Mobility and Handover

This section is based on [11] and [18].

Users expect from small-cells the same service experience that they have grown accustomed to with macro cells. Therefore, a seamless transition from macro cells to small-cells is essential. Mobility coordination among multiple neighbouring small-cells is also critical for the operators to moderate the complexity of the network, especially for the case of independent user-deployed small-cells.

In HetNets due to the small-cells' limited coverage, there can be an excessive number of handovers. Therefore, mobility management of UE is a key requirement for feasibility of HeNB deployment in LTE networks.

Generally, there are two handover scenarios that can be found when both macro cells and small-cells are deployed together, as seen in Figure 2.12.

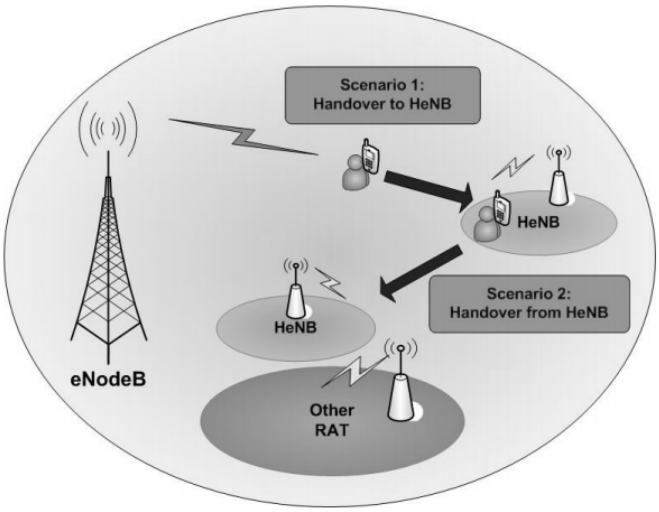

Figure 2.12: Different Types of Handovers in HetNets (extracted from [18]).

The first handover scenario is an inbound handover from a macro cell to a small-cell or HeNB. In the second handover scenario, the UE is connected to a HeNB and performs the handover either to a small-cell, macro cell or other Radio Access Technologies (RAT).

The handover from a macro cell to a small-cell is quite demanding and complex. One of the challenges in this handover procedure corresponds to the decision mechanism since there are hundreds of possible targets. LTE uses a network-controlled and UE assisted handover procedure for macro cells. This means that the UE measures the downlink signal strength and sends the measurement report to the serving eNB. The serving eNB then makes the handover decisions based on the received measurement reports.

The common metrics used in the handover decision mechanism include Carrier to Interference-and-Noise Ratio (CINR), Receive Signal Strength Indicator (RSSI) and QoS. However, considering the increased number of handovers that occur in HetNets such metrics are too demanding to be implemented. Another factor to consider is the case of small-cells with a CSG which will not be able to be accessed by macro cells. A high quantity of measurements for non-allowed CSG cells should be avoided. If the

UE measures all the HeNBs and reports the measurements to the serving eNB, it will consume too much power which will affect the battery life and cause handover delay. Consequently, other parameters should be considered to optimize the handover procedure like: service cost, interference level, load balancing and speed status of the UE.

The speed status of the UE is relevant because 3GPP specifies small-cells enhancements for both indoor and outdoor deployments. For indoor UE, only low UE speed ($0 - 3$ km/h) is targeted. For outdoor, medium UE speed (up to 30km/h and potentially higher speeds) are also targeted. If a UE is moving at a higher speed the number of handovers will increase considering the small-cells' low coverage area so it might be more useful for the UE to be served by the macro cell, in such scenario.

The handover process between small-cells is similar to the procedure just discussed because the UE will face hundreds of possible targets.

The handover procedure from a small-cell to a macro cell eNB is relatively simple. The UE has one obvious option as the target cell, the macro cell eNB with the highest RSSI. When the RSSI from the eNB is stronger than the small-cells' RSSI, the UE will be connected directly without a complex interference calculation or authorization check.

2.3 Propagation Models

This section is based on [19], [20] and [21].

The overall objective of mobile operators is to satisfy users' needs with adequate coverage and QoS. The performance of wireless communication systems depends in a fundamental way on the mobile radio channel. Consequently, predicting the propagation characteristics between the transmitters and receivers is crucial for the design and installation of a radio network communications system. To do this, calculations and optimisation procedures are constantly taking place. All computations and simulation procedures depend on reliable propagation models. A propagation model is a formulation that intends to characterise and predict radio wave propagation. The basis for any propagation model is a database, which describes the propagation environment. The geographical databases are used alongside the propagation models in the radio network planning process. They contain information on the terrain and the obstacles found between the transmitter and receiver and are a compulsory requirement when using sophisticated prediction tools.

The deployment of small-cells results in HetNets that have a more complex topology than the usual homogeneous networks. The traffic demand is non-uniform because of the hotspots and the short coverage radius of small-cells. Therefore, choosing an appropriate propagation model and using an database that realistically depicts the environment is of great importance to accurately predict path-loss for Line of Sight (LOS) and Non Line of Sight (NLOS) conditions.

2.3.1 Types of Propagation Models

Several propagation models have been developed and proposed for cellular systems operating in different environments (outdoor, urban, suburban, rural, and indoor) but there are generally three different types of propagation models: empirical models, deterministic models and semi-empirical models. Stochastic models are also sometimes considered as a fourth category of propagation models, as represented in Figure 2.13.

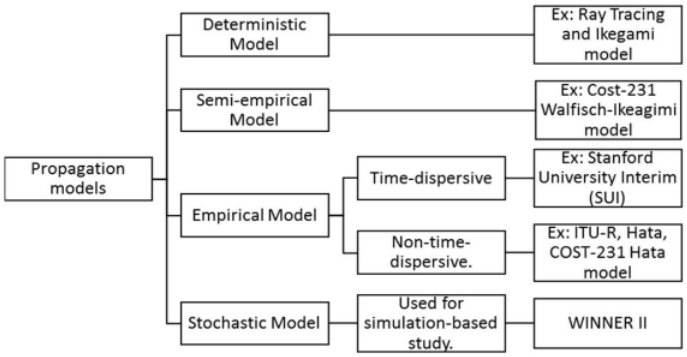

Figure 2.13: Types of Propagation Models (extracted from [22]).

A stochastic model represents the environment as a series of random variables, therefore it requires less information about the environment and less processing power. The WINNER II model commonly used in 3GPP simulations assumes that most of the multipath components arrive close to the plane that contains the antenna and ignore the variation in the elevation plane. This assumption is not valid in small-cell environments where narrow beams could be used to cover multi-floor buildings and multipath components could arrive from any direction not just in azimuth plane. [23]

An empirical model is based on observations and measurements. These are useful to study the general behaviour or to enable a rough estimation of the number of required cells in a large area. The classification of empirical models can be further divided into time dispersive and non-time dispersive. Time dispersive provides information about time dispersive characteristics of the channel, like the multipath delay spread of the channel. Non-time dispersive models consider various parameters, such as distance, antenna heights, frequency and transmitter power to predict average path loss. [22]

The Okumura Model and the Okumura-Hata Model were some of the first empirical models developed that served as groundwork to many others. The COST-231 Hata Model, based on the previous ones, is another commonly used empirical model.

The Standard Propagation Model (SPM), used in radio network planning software, is a propagation model based on formulas of Okumura and Hata that was adapted to perform signal coverage predictions in the frequency range of 150 MHz to 3500 MHz and for distances between 1 km to 20 km. The SPM is best applied on mobile technologies such as LTE and LTE-A.

Semi-empirical are based on a combination of measurements and theory and attempt to interpret field data based on theoretical principles. The first site-specific propagation models were semi-empirical and were based on detailed terrain characteristics extracted along the individual propagation paths be-

tween transmitter and receiver. These models use low resolution geographic data but still manage to obtain reasonably fair results for coverage predictions in urban areas. They are, however inefficient when it comes to indoor coverage estimates in dense urban areas. The COST 231 Walfisch-Ikegami is considered a semi-empirical model used to predict urban environments. This model is an extension of COST-231 Hata model and it can be used for frequencies above 2000 MHz. [24]

Deterministic models are numerical methods that simulate radio waves propagation by reproducing the physical propagation phenomena. They use the geographical and morphological information from a database for a deterministic solution of Maxwell's equation to determine the received signal power. These models use a specific location for the transmitter and the receiver to provide a reliable and thorough estimation of the path losses and the channel characteristics. They rely on terrain descriptive features (altitude, the geometry of the buildings, materials used in construction) to simulate the shadowing effect that a signal experiences to provide a correlated spatial variation of the path loss.

There are two different types of deterministic models: vertical-plane models and ray-based models. Most vertical-plane models used alongside radio planning tools are based on multiple knife-edge diffraction scenarios. Vertical-plane models are bi-dimensional and only analyse the direct path of the transmission. On the other hand, ray-based models use the ray-optical approximation, which is based on Geometrical-Optics and on the Uniform Theory of Diffraction. These models describe the propagating field as a set of rays undergoing multiple reflections and diffractions from the obstacles in the propagation environment. They predict with high accuracy the field strength around low transmitters in urban environments. [25]

Comparing the simulation results of a vertical-plane model with the ones from a ray-based methodology, as it is done in Figure 2.14, one can conclude that the ray-based model more precisely illustrates the coverage area surrounding the small-cell. However, ray-based prediction methods like ray tracing require detailed input parameters and high resolution geographical data which will contribute to increased computational complexity and therefore restrictions when it comes to widespread usage.

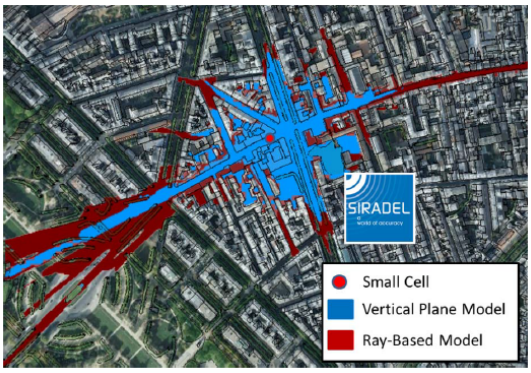

Figure 2.14: Comparison of a VP Model and a Ray-Based Model (extracted from [19]).

Ray tracing was established as a promising environment emulator for studying channel characteristics in urban environments. This technique allows fast computation of single and double reflection processes, and also does not require ray splitting. On the downside, effort increases exponentially with the order of reflections that are included in the simulation. [26]

One ray tracing model worth mentioning is the Intelligent Ray Tracing (IRT) model. This model was developed to overcome the computational demand of other ray tracing models. It computes for each valid path between transmitter and receiver the corresponding path loss but unlike other ray tracing models the building database used is pre-processed, leading to computation times in the range of empirical models. As urban areas are characterized by multi-path propagation and subject to reflection, scattering and diffraction at walls, edges of buildings and similar obstacles the IRT model also considers the losses due to reflections and diffractions. A comparison between a prediction with the Okumura-Hata model and a prediction with the IRT model is presented in Figure 2.15.

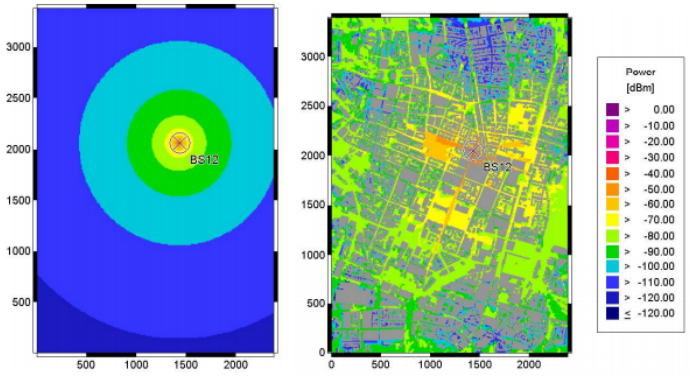

Figure 2.15: Predictions with Hata-Okumura Model (left) and IRT Model (right) (extracted from [27]).

The equation 2.1 describes the path loss for a IRT model:

$$L = L_{FS} - G_T + L_{interaction} = 32,45 + 20log_{10}(f) + 10nlog_{10}(d) - G_T + L_{interaction} \tag{2.1}$$

where:

- f: frequency in MHz;
- n: path loss exponent depending on the propagation situation;
- d: distance between the transmitter and receiver in kilometres;
- G_T: gain of the transmitting antenna;
- $L_{interaction}$: losses in the propagation path due to reflection, diffraction or phenomena.

The pre-processing is done by firstly dividing the walls of the building (or other obstacles) into tiles and the edges into horizontal and vertical segments, as represented in Figure 2.16. After this, the visibility conditions between these different elements (possible rays) are determined and stored in a file that includes the occurring distance, as well as the incident angles. Figure 2.16 also represents an example of a ray path between a transmitter and a receiver with a single reflection.

The result of this pre-processing can be represented by a “visibility tree”, as depicted in Figure 2.17. When the transmitter location changes, only the uppermost branches in this tree must be computed again, to determine which elements are in the LoS of the transmitter. Consequently, all the other relations only have to be computed once. So basically the computational demand of each prediction is reduced to

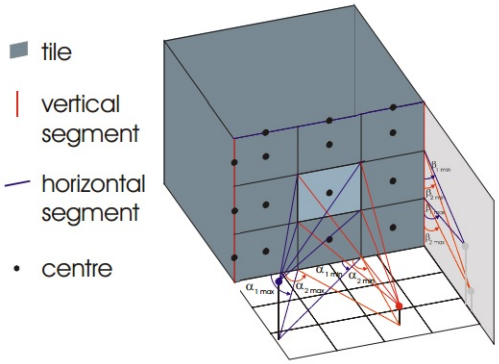

Figure 2.16: Tiles and Segments of a Wall (adapted from [28]).

the search in the tree structure. This tracking is done until the receiver is reached or a maximum number of interactions (reflections and/or diffractions) is exceeded.

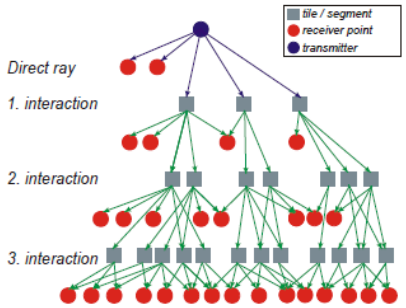

Figure 2.17: Tree Structure Representing All the Visibility Relations (extracted from [28]).

The IRT model groups the different combinations of possible rays into path classes according to how many interactions should be considered for the determination of rays between transmitter and receiver. Within a specific class the different rays are assumed to experience a similar interaction loss and as the order of the path class increases so does the loss values. The default value for maximum number of path classes considered is 8, as represented in Table 2.1. Lower values accelerate the prediction to some extent and the usage of higher path classes increases only the consideration of the wave guiding effect.

Table 2.1: Classification of the Different Rays Into Path Classes (extracted from [27]).

Path Class	Description
1	Direct Path
2	Single Reflection
3	Double Reflection
4	Single Diffraction
5	Triple Reflection
6	One Reflection + One Diffraction
7	Double Diffraction
8	Two Reflections + One Diffraction

The Dominant Path Model (DPM) is another type of propagation models widely used in radio network planning. A DPM does not rely only on the direct ray (like empirical models) and it does not consider hundreds of rays for a single radio link (like ray tracing), as pictured in Figure 2.18. Instead it focuses on the most dominant path between transmitter and receiver. The Urban Dominant Path (UDP) model is one of the dominant path models that was developed for the prediction of the field strength specifically in urban environment.

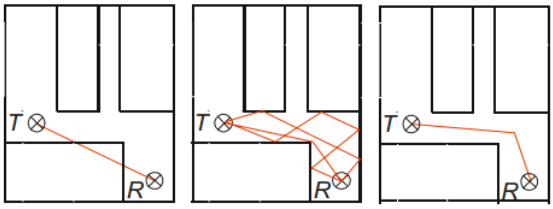

Figure 2.18: Empirical models (left), Ray Tracing (middle) and DPM (right) (extracted from [29]).

The algorithm of DPMs can be resumed in two different stages. Firstly, the dominant paths have to be determined and then the prediction of the path loss for each path must be calculated. Initially, the location of the transmitter, receiver and surrounding obstacles is used. A transmitter (T), a receiver (R) and the different types of corners are portrayed in Figure 2.19. The dominant path must lead via convex corners from the transmitter to the receiver. For the determination of the path, a tree with all convex corners is computed starting with the corners visible from T.

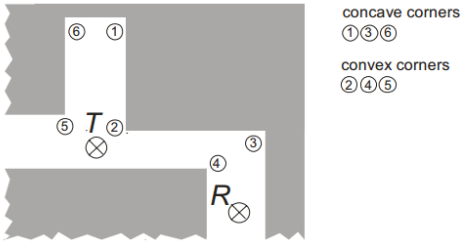

Figure 2.19: Transmission Scenario (extracted from [29]).

Every convex corner visible from the examined corner is a new branch in the tree, as shown in Figure 2.20.The algorithm for the determination of the dominant paths leads to more than one solution. However in the majority of the cases one solution with the smallest path loss is enough for an accurate prediction. This one solution is called Minimum Loss Dominant Path (MLPD). The MLDP is chosen by comparing the prediction path losses of the different paths. [30]

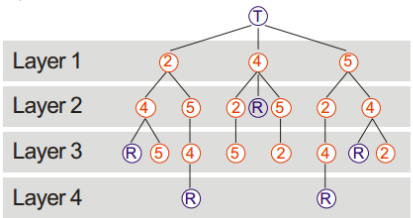

Figure 2.20: Tree Structure of the Scenario Depicted in Figure 2.19 (extracted from [29]).

The prediction of the path loss (PL) of a path with length d is calculated in dB, with equation 2.2:

$$PL = 20log_{10}(\frac{4\pi}{\lambda}) + 10plog_{10}(d) + \sum_{i=1}^{n} f(\varphi, i) + \sum_{j=1}^{m} T_j - \Omega \tag{2.2}$$

where:

- λ: wavelength;
- Ω: wave guiding factor;
- f (φ,i): function which determines in dB the loss due to the change in direction of propagation.

The angle between the former direction and the new direction of propagation is φ. The factor "p" depends on the visibility between the current pixel and the transmitter. By adapting "p" to each situation, different path loss exponents and individual breakpoints depending on the LOS or NLOS condition are enabled. To determine the path loss in indoor scenarios, transmissions through walls have to be added. T_j represents the transmission loss of wall number j, where T_2 would be the transmission loss of the second wall penetrated by the dominant path.

The UDP model also takes into account the topography of the environment studied as this might influence the visibility between the examined points. This model also offers advantages in scenarios where the antenna location is above the mean building height, as it is less sensitive to the inaccuracies caused by the simplification of the diffractions at rooftops. The model is suitable for extremely large scenarios, where predictions with ray tracing models are still not possible. Studies have shown that the accuracy of the UDP model exceeds the accuracy of ray tracing. [29]

2.3.2 Types of Databases

As mentioned above, propagation models perform their predictions using information from terrain databases. The environment to be analysed and predicted is stored in a database file. But depending on the type of scenario (indoor, urban or rural), the resources available and the overall level of accuracy intended for each project a different description of the relevant obstacles is necessary.

The most rudimentary type of database used nowadays is a 2D database. It is composed by a height file or Digital Terrain Model (DTM) and a clutter file. The DTM consists in a digital model that represents the surface of the Earth, excluding vegetation as well as buildings and man-made structures. It contains the altitude values of the region and as such is characterized by a latitude Y, a longitude X and a specific resolution. The resolution is linked to the retrieval of the topographic data according to a given scale.

The clutter file used in a 2D database describes the land use classification of the area in analysis including any features that impact the radio wave propagation. The clutter types or so-called clutter classes include natural environments: river, forest, ocean or man-made: industrial, suburban, dense urban, to name a few. The appropriate number of clutter classes depends on the geographic area. The combination of the DTM and the clutter types result in a 2D database because the altitude only refers to the height of the terrain and no clutter height information is usually provided. The propagation models

that use 2D databases are empirical ones. In empirical models the path loss is calculated for the direct path between the transmitter and receiver and the topography of the terrain is only used to calculate obstructions. According to the given clutter category of the area, an attenuation or gain is added to the total path loss.

Another type of database used is a 2.5D database. While it also consists of a DTM and clutter categories it includes the average height of each scenario by introducing the clutter heights. Each specific category will have a preassigned average height, for example a low density urban area will have an average height of 20 metres and an area classified as a village might have an average height of 6 metres.

If a higher accuracy is necessary, subcategories with a specific height assigned to it can be created within a clutter class. This method provides with a better correspondence with the real environment. For example, a scenario labelled as dense urban can be divided in two, one with an average height of 15 metres and the other with 20 metres. The most comprehensive and detailed type of database is a 3D database. Like previous databases it uses a DTM and clutter types (it may or may not include the clutter heights) but incorporates the height and contour of the buildings (3D Building Vectors). When using a 3D database, each of the buildings will have its own height and shape represented as close to reality as possible, unlike previous databases.

If we consider a 2D database and assume it has a resolution of 5-20 metres, a 2.5D database would have a resolution in the range of 5-10 metres and a 3D database would have a resolution of 1-5 metres, for comparison purposes. [31]

Most of the current propagation models are dedicated to a single scenario (either urban or indoor) and interferences between indoor and outdoor transmitters cannot be computed with the required high accuracy. In urban scenarios, the databases usually have limited 3D information, so they are categorized as 2.5D. Each building is represented as a polygonal cylinder with its ground plane and a uniform height. The material properties of each building can be defined individually or default properties for all buildings can be used if no detailed information is available. In contrast to the urban case, the indoor database consists of polygons with arbitrary shapes and orientations. The highly accurate definition of an arbitrary number of objects with different materials is possible. Additionally, subdivisions with different material properties can be modelled.

2.4 State of the Art

This section addresses the studies related to LTE networks using small-cells and propagation models used in such deployments. The studies presented relate to urban environments, which is the framework of this thesis.

In [32], a study about the coverage performance of different LTE network topologies is presented. Simulations are performed in a typical dense urban environment with macro-cells, small-cells both together and isolated, to analyse spectral efficiency and the network capacity improvement. The authors use radio-planning simulation tools to assess small-cell deployment coverage and performance. First,

an accurate description of the environment is achieved by using high-resolution geographical map data and site specific path-loss models. These methods allow for the prediction of in-street canyoning and realistic outdoor-to-indoor propagation. Subsequently, LTE downlink metrics (SNR and spectral efficiency) are simulated. The simulation is conducted by defining multiple DL traffic loads and introducing 3D path-loss matrices, obtaining results at each UE location. The 3D feature of the study relates to the fact coverage maps are calculated for users located in the streets and different building floors. The result is, as expected, higher floors have less macro-cell coverage, inducing less interference in small-cells communications. After analysing the coverage statistics of the different environments and considering both indoor and outdoor static users, it concludes that the worse spectral efficiency is obtained by using macro-cell only coverage. The small-cells deployed as a complement to the macro layout significantly improve the spectral efficiency. The small-cell only network gives an even larger spectral efficiency however it cannot be considered as satisfactory since part of the indoor locations are not covered. The authors conclude that the optimisation of a HetNet is a challenging task because the performance is highly sensitive to the traffic demand and the number of parameters to be adjusted is large. Also, in order to obtain clearer conclusions on network optimisation additional simulations are required.

The authors in [33] after presenting the features and functionalities of small-cells, focus on the challenges encountered in small-cells deployments in real-life networks and discuss a methodology to deal with them. The first challenge identified relates to the location of the small-cells so that maximum traffic is captured. The next constraint discussed is how to minimise interference with macro cells and lastly how to minimise the overall deployment costs.

According to the methodology presented, the first step in designing HetNets is to identify traffic hotspots areas. This step is crucial as multiple studies have shown that around 50% of the volume of traffic is concentrated in small geographic areas in urban environment. Also, according to the authors, 70-80% of mobile data traffic is generated indoors in nomadic conditions. In addition, often 20-30% of mobile data subscribers generate 40-50% of data traffic.

Furthermore, the amount of traffic captured by a small-cell should be estimated as it depends on the transmit power of each cell and cell re-selection and handover parameters. In case of using a shared carrier, the footprint of the cell also depends on the relative strength of the macro cell compared to the small-cell. The following step should be to evaluate the amount of capacity growth that can be absorbed by the existing network. Then, two options should be developed: the first one will only grow the current macro network and the second will add capacity through a HetNet. The best alternative is the one that satisfies the capacity growth and has a minimum relative cost.

To conclude, the authors emphasise the need to include QoE as a basic constraint in the design of networks. It has been observed that the total traffic on the network has had a significant increase after the deployment of small-cells which shows an unfulfilled demand in existing networks. By strategically choosing the location of small-cells to cover the weak coverage spots of the macro cell and the fact that the number of simultaneous users in a small-cell footprint is relatively small and are in more favourable LoS conditions are the main reasons which contribute to a better user experience in HetNets.

The work presented in [34], investigates and compares the DL performance of several different types

of small-cell deployments by using realistic 3D building maps to model the indoor traffic distribution and a ray-tracing tool to evaluate path loss and antenna pattern effects.

The investigated deployment schemes are outdoor pico-only, indoor femto-only and joint pico-femto deployments, all combined with the existing macro layer. A minimum required user data rate of 1 Mbps was defined and for the original macro only deployment 43% of the users were in outage and that 70% of those users were located indoor. The objective is to effectively decrease the outage level to 10% and for that the small-cells are to be deployed on dedicated channels that do not interfere with the macro layer.

The study concludes that a pico-only deployment with 3 outdoor picocells per macro sector, or alternatively an indoor femto-only deployment with a density of 400 femtocells/km^2, is sufficient to fulfil the outage target and to offload 50% of the users. Although the indoor femto-only scenario gives the best performance in terms of average user throughput, the hybrid deployment of outdoor picocells and indoor femtocells - with each layer transmitting on dedicated frequency resources - gives similar capacity improvements at a lower base station density and 70% of offloaded users.

A study related to picocell propagation in urban environments contemplating ray tracing software was made in [35]. The main objective of this study is to derive a set of urban 3D picocell propagation statistics suitable for LTE HetNet planning. The authors studied two different urban environments: a 17.6 km^2 area in the city centre of Bristol, UK, and a 143 km^2 area in the centre of London, UK where a large number of picocell BSs and users were randomly scattered. There were two different picocell BS antenna mounting options modelled. The picocell BS antennas mounted on external walls of buildings were directional patch antennas and the picocell BS mounted at lamp-posts were omnidirectional dipoles that illuminate a circular area. All the analysis was performed at 2.6GHz with a transmit power of 30dBm. The study indicates that large datasets of picocells in two urban environments do not have major statistical differences between each other. In contrast, it was noted that the propagation statistics depend significantly on the mounting option. When a pico BS is mounted on the side of a building, the received signal strength is stronger than the lamp-post mounting option by up to about 5dB for the LOS and about 10dB for the NLOS links. A suggested cause for this behaviour is the existence of strong reflections on the wall on which the BS is mounted. The results also showed that the received signal strength decays with distance and the shadowing is greater for the NLOS links, as expected.

In [36], the authors focus on simulating urban propagation models using WinProp, the propagation prediction software. The simulations are performed at 2.4GHz in an urban environment with an omnidirectional transmitter. After a brief description of the models used, the COST 231 Walfisch-Ikegami, the Intelligent Ray Tracing and the Dominant Path Model, the results of the simulations are presented and compared. From the three models, the COST 231 Walfisch-Ikegami is the one most suitable for short distances as it obtained the highest value of received power, -27 dBm, in the first 40 metres while the IRT obtained -47.72 dBm and the DPM obtained -52.73 dBm. However, the DPM simulation showed an improvement in the final stretch and by the end of the 1600 metres it obtained the highest value of received power with -100.98 dBm. The work concludes that the DPM overcame the initial propagation problems and started to propagate the signal well after about 800 metres.

The work presented in [37], proposes a new concept based on dominant paths that aims to predict the field strength in hybrid scenarios. This new approach allows the computation of the transition from an urban to an indoor scenario and vice versa, by allowing a combination of the UDP and the Indoor Dominant Path (IDP) models. The transition interface is described and the need for two different types of databases and a smooth transition between environments is emphasised. The model is described as capable of handling objects with arbitrarily located and rotated planes, as well as very large areas. One should note that the prediction in an urban area is done on one height level, whereas in the indoor environment multiple prediction layers can be considered during the computations. To validate the model, several comparisons between theoretical predictions and real measurements were performed in urban, indoor and combined environments. The outcomes confirmed that the model delivers very accurate results.

Chapter 3

Methodology

This chapter presents the methodology used in this work. Firstly, some context is given to understand the general scope. The propagation models tested are then presented and a brief description of the data used and the corrections that had to be implemented are also stated.

3.1 Context

The requirement of higher throughputs and capacity in mobile communications prompted the development of new solutions, like the case of small-cells. However, not only did the solutions implemented suffered changes, but the methods used for planning and optimising the networks have had to evolve. The increased complexity of mobile networks particularly in highly populated urban areas has made some propagation models and corresponding databases rather obsolete or inaccurate. Consequently, adjustments had to be made to existing models and new ones were developed. Currently, acceleration techniques and simplifications to these methods are constantly taking place in order to optimise computation times.

In the present work, the analysis of several propagation models using different types of geographical databases will be performed. Each propagation model will be adapted to the specific geographical database that is used in each case, starting with the most basic one to the most complex one. The area of interest is situated in the centre of Antwerp, a city in Belgium. This area is served by 12 Macro LTE sites, as presented in Figure 3.1.

The analysed network and data were provided by a Belgium operator for a project Nokia was involved that studied the coverage improvement of that urban area with the deployment of small-cells. The conducted walk test collected received signal strength data alongside a pre-planned survey route. The computation of the propagation models and respective coverage predictions will be performed using 9955 RNP, a Nokia software for radio network planning. The results of each prediction will be compared to real data obtained in a walk test.

The main goal is to conclude what is the best combination of propagation model and type of database for this specific case. Nevertheless, seeing as the cost of each database should be considered in a real

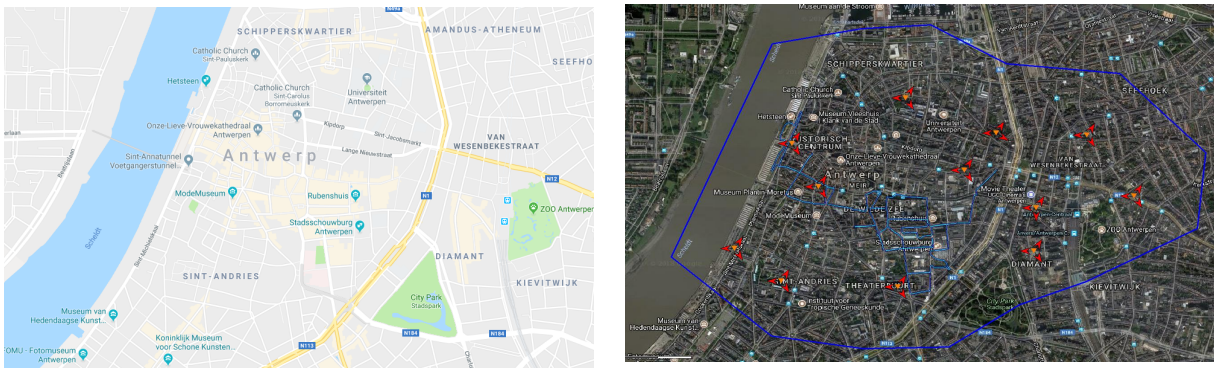

(a) Antwerp in a map

(b) Area considered

Figure 3.1: Area analysed

project, it would be useful to obtain some general conclusions regarding the use of the same propagation model with different types of databases in this type of environment.

The first step to obtain accurate predictions using each of the propagation models, is to configure the existing network in the 9955 tool. The area is served by 12 sites operating at 1800 MHz. First, the table that contains the information regarding each site is filled in. The mandatory fields include the name, latitude and longitude of each site. After adding each of the sites, a table called Transmitters has to be completed. This table contains information regarding every single base station of each site. Some parameters that need to be configured include the antenna model, the height of the antenna mast, the azimuth, the mechanical and electrical tilt, the cable losses and the specific propagation model to be used. The remaining parameters like the frequency band, maximum power or use of diversity are included in the Cells table. The common parameters of the base stations in each site are depicted in Table 3.1.

Table 3.1: Parameters of Transmitters

Transmitter	Frequency Bands	Antenna Height (m)	Cable Losses (dB)	RS Power (dBm)
A	1800 FDD - 20 MHz	27.6	0.65	13.9
B	1800 FDD - 20 MHz	43.3	3.2	16.9
C	1800 FDD - 15 MHz	36.5	1.98	16.4
D	1800 FDD - 15 MHz	30.52	0.65	16.4
E	1800 FDD - 20 MHz	29.7	2.62	13.9
F	1800 FDD - 15 MHz	18.5	1.45	18.5
G	1800 FDD - 15 MHz	22	0.65	16.4
H	1800 FDD - 15 MHz	19.9	0.65	12.4
I	1800 FDD - 15 MHz	44	0.65	13.9
J	1800 FDD - 20 MHz	22.5	0.65	13.9
K	1800 FDD - 20 MHz	28.6	0.54	13.9
L	1800 FDD - 15 MHz	29.25	0.79	12.4

3.2 Propagation Models Used

The first model applied is the Okumura-Hata model. This model established empirical mathematical relationships which described the graphical information of the Okumura model. The equation 3.1 describing the average path loss in an urban area is given by:

$$PL = 69.55 + 26.16log_{10}(f) - 13.82log_{10}(h_T) + [44.9 - 6.55log_{10}(h_T)]log_{10}(d) - H(h_R, f) \quad (3.1)$$

where:

- f: frequency in MHz;
- H_T: transmitter height in metres;
- d: distance in kilometres;
- H(h_R,f): correction factor for the mobile antenna height.

The correction factor is computed differently according to the size of the area in question. In this case:

$$H(h_R, f) = \begin{cases} 8.29(log_{10}1.54h_R)^2 - 1.1, f \leq 200MHz \\ 3.2(log_{10}11.75h_R)^2 - 4.97, f \geq 400MHz \end{cases} \quad (3.2)$$

where:

- f from 150 MHz to 1500 MHz;
- h_T from 30 m to 200 m;
- h_M from 1 m to 10 m;
- d from 1 km to 20 km.

This model will only be applied with a 2D database as it is empirical.

The COST 231 – Hata Model will also be used. This model extends the previous one to cover the frequency range of 1500 MHz to 2000 MHz. The other validity conditions are maintained.

The path loss is given by:

$$PL = 46.3 + 33.9log_{10}(f) - 13.82log_{10}(h_T) + [44.9 - 6.55log_{10}(h_T)]log_{10}(d) - H(h_R, f) + C_m \quad (3.3)$$

where:

$$H(h_R, f) = \begin{cases} 8.29(log_{10}1.54h_R)^2 - 1.1, f \leq 300MHz \\ 3.2(log_{10}11.75h_R)^2 - 4.97, f \geq 300MHz \end{cases} \quad (3.4)$$

$$C_m = \begin{cases} 0dB, \text{for a medium-sized city and suburban areas} \\ 3dB, \text{for metropolitan areas} \end{cases} \quad (3.5)$$

Similarly, to the Okumura-Hata model, the predictions using the COST 231 – Hata Model will only use a 2D database given its empirical nature.

The SPM will also be tested. The model is based on equation 3.6 and each of the K parameters can be adjusted according to specific conditions such as terrain profile, diffraction mechanisms, morphology of clutter classes and the effective height of the transmitting and receiving antennas. [38]

$$P_R = P_T - [K_1 + K_2 log_{10}(d) + K_3 log_{10}(hT) + K_4.DiffractionLoss + K_5 log_{10}(d).log_{10}(h_T) + K_6 h_R + K_7 log_{10}(h_R) + K_{CLUTTER}.f_{CLUTTER} + K_{HILL}] \quad (3.6)$$

where:

- P_R: received power in dBm;
- P_T: Effective Isotropic Radiated Power (EIRP) in dBm;
- h_T: effective height of the transmitter in metres;
- h_R: effective height of the receiver antenna in metres;
- d: distance between the receiver and the transmitter in metres;
- Diffraction Loss: losses due to diffraction over an obstructed path in dB;
- $f_{CLUTTER}$: weighted average losses due to the clutter.

The specific recommended adjustment coefficients will not be presented as they are classified by Nokia as internal use only. The SPM will be used with the 2D and 2.5D database and the formula will be adapted for each one according to Nokia's internal guidelines.

For the coverage prediction using a 2D database, 9955 computes the total path loss using the topographical information of the terrain provided in the DTM files, as shown in Figure 3.2 and the clutter class of the area.

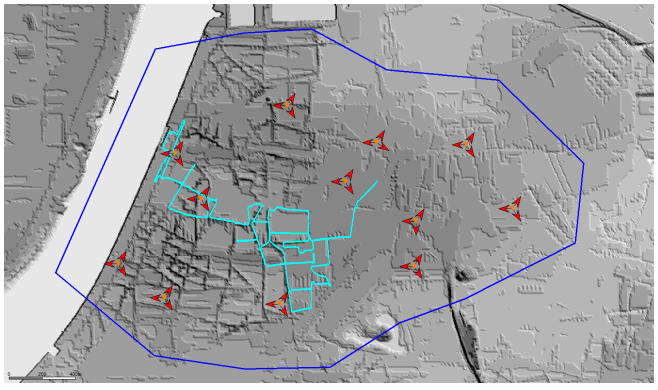

Figure 3.2: DTM representation in 9955

Each clutter class will have assigned a specific loss value that is then added to the total path loss equation. The loss values used correspond to Nokia internal guidelines. [39] The clutter classes that had a relevant representation in the polygon area are presented in Table 3.2. The Habitation, Industry and Monuments classes were given the same colour scheme (that ranged from light grey to black as the

height of the constructions increased) despite being different clutter classes to portray more accurately the area in terms of height. There are two different categories of areas: the polygon area and the buffer area. Both areas are represented in terms of surface and percentage occupied by each clutter class.

Table 3.2: Clutter Classes and Distribution

Clutter Classes	Polygon Area		Buffer Area	
	Surface (km^2)	Percentage	Surface (km^2)	Percentage
Open Area	1.954575	43.1	0.04208	92.9
Tree	0.019	0.4	0.0004	0.9
Shack	0.001	0	0	0
Shack	0.39605	8.8	0	0
Wood $<$ 12 m	0.00093	0	0	0
Wood $>$ 12 m	0.03035	0.7	0.00007	0.2
Habitation $<$ 12 m	0.6614	14.6	0.0005	1.1
12 m $<$ Habitation $<$ 25 m	1.08662	24.1	0.00217	4.8
25 m $<$ Habitation $<$ 40 m	0.09763	2.2	0	0
Habitation $>$ 40 m	0.00355	0.1	0	0
Industry $<$ 12 m	0.05335	1.2	0	0
12 m $<$ Industry $<$ 25 m	0.02593	0.6	0	0
25 m $<$ Industry $<$ 40 m	0.00573	0.1	0	0
Industry $>$ 40 m	0.00015	0	0	0
Monument $<$ 12 m	0.02382	0.5	0.00007	0.2
12 m $<$ Monument $<$ 25 m	0.07255	1.6	0	0
25 m $<$ Monument $<$ 40 m	0.05212	1.2	0	0
Monument $>$ 40 m	0.01085	0.2	0	0
Road Bridge	0.0023	0.1	0	0
Rail Bridge	0.00543	0.1	0	0
Embankments	0.00222	0	0	0

The polygon area corresponds to the area inside the dark blue polygon, shown in Figure 3.3 and represents the centre of the city. The buffer area is represented in light blue in Figure 3.3 and it corresponds approximately to the path taken while performing the walk test. In the background of Figure 3.3 the clutter classes are also represented. Each building or structure is coloured according to its clutter class.

To compute the predictions with the 2.5D database, 9955 will use the path loss formula and added losses according to the clutter class like in the previous case but it will also consider an average height for each clutter class, on top of the terrain topography. The specific height given to each clutter class

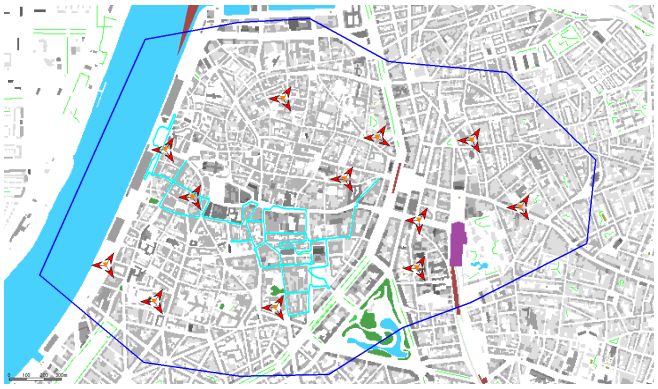

Figure 3.3: Polygon and Buffer Area

was also defined after analysing Nokia's internal guidelines.

The main difference between a 2.5D and a 3D database consists in the building vector file. The vector file describes each building height, shape and orientation in detail. The visual representation of the building vector is represented in Figure 3.4.

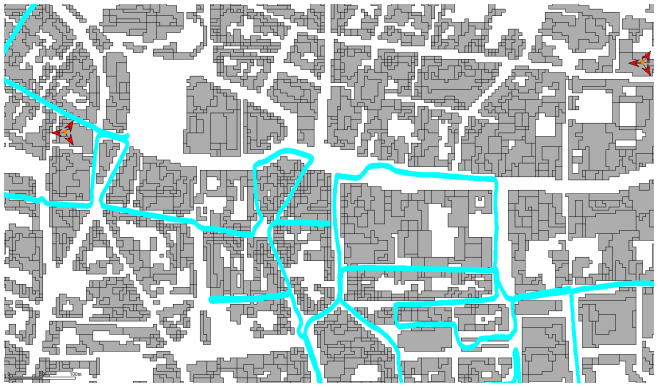

Figure 3.4: Building Vectors

Another propagation model tested was the WinProp UDP. This model is known to be a trade-off between computation complexity and accuracy. As previously mentioned, UDP model focuses on the dominant path between transmitter and receiver instead of computing hundreds of paths each with small contributions. The 3D building database was pre-processed prior to the prediction computation, using Wallman a module that is part of the WinProp wireless network planning software package.

In conclusion, the propagation models used and the corresponding databases are listed in Table 3.3.

Table 3.3: Propagation Models and Databases Tested

Model	2D Database	2.5D Database	3D Database
Okumura – Hata	X		
COST 231 – Hata	X		
SPM	X	X	
WinProp UDP Outdoor			X
WinProp UDP Indoor			X

3.3 Data Adjustments

Some corrections had to be implemented to reduce any inconsistencies in the data obtained in the walk test and to make it comparable to the results of the predictions obtained with 9955.

The buffer area, used in the coverage analysis by area, is represented in more detail in light blue in Figure 3.5.

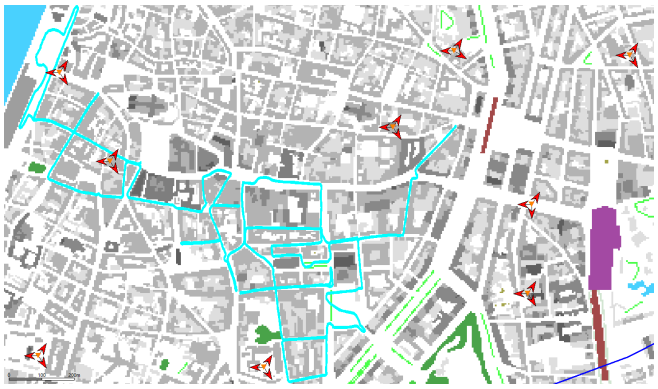

Figure 3.5: Buffer Area

This buffer area was created by analysing and connecting each position of the walk test to create a path. After the path was created, it was transformed in an area using QGIS. This area has an average width of 8 m and will serve as the total area used for each coverage prediction. As seen in Table 3.3, by using the buffer most of the area analysed is categorized as Open Area which corresponds to the actual streets. Considering 9955 adds a specific loss value according to the clutter class, if this correction was not performed, the values of the predictions would be over-estimated because they would include the loss value associated to each building or other obstacles. This method attempts to reduce possible errors resulting from the comparison of the real data and the predictions obtained by 9955. Therefore it will make the coverage predictions better correspond to the coverage at street level.

It is relevant to add that any errors found while analysing the walk test points were also corrected. This means any walk test location that was shown to be in an indoor situation was placed in the nearest possible outdoor position, since it is known the walk test only took place outdoors. As this is a dense urban environment, this occurred quite frequently especially in narrow streets. An example depicting the adjustment of the walk test points is shown in Figure 3.6 where the yellow points correspond to the GPS position of the walk test and the light blue to the buffer.

The data obtained in the walk test was also treated to eliminate any inconsistencies. If at a given point, with the same coordinates, different signal values were recorded by the same transmitter an average value was then used.

The measurements recorded during the walk test include the RSRP and RSRQ. The RSRP is the average of power levels received across all reference signal symbols within the considered measurement frequency bandwidth. The Reference Signal Received Quality (RSRQ) is the ratio of RSRP and the E-UTRA Carrier Received Signal Strength Indicator (RSSI). The E-UTRA carrier RSSI comprises the total received wideband power observed by the UE.

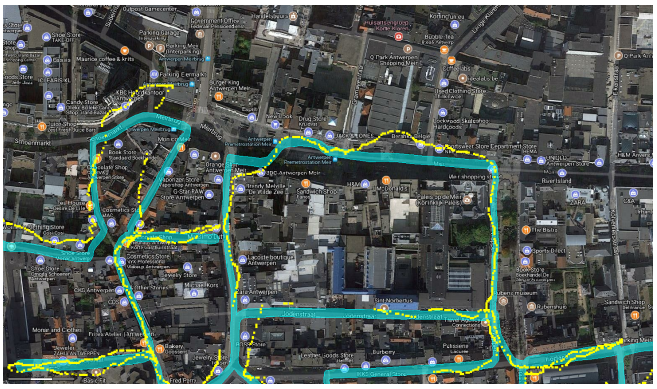

Figure 3.6: Correction of Walk Test Points

The signal values recorded during the walk test correspond to the signal level from the best server, that is the signal level obtained at any given moment is always the strongest one received from all the transmitters. The coverage predictions run by 9955 also considered the signal level of the best server to keep the coherence with the walk test data.

Chapter 4

Results

This chapter starts with a brief description of the scenarios tested. Results were separated into two categories: an analysis in terms of area and point-to-point. Coverage results for each model are presented separately and then the comparison of the results of the different propagation models concludes the chapter.

4.1 Coverage Results by Area

4.1.1 RSRP Coverage Results

After managing the results of the walk test to reduce any inconsistencies, they were added into the 9955 tool. This procedure allows to represent them graphically and to compare their geographical position to the buffer area used in the coverage predictions of the different models.

In Figure 4.1 the RSRP results of the walk test are presented. The scale goes from RSRP levels higher or equal to -55 dBm to RSRP levels higher or equal to -115 dBm, with a step of 5 dB.

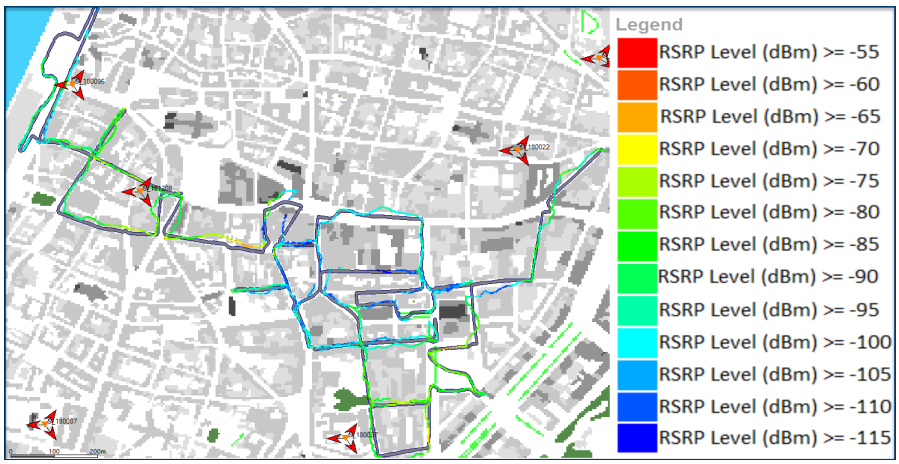

Figure 4.1: RSRP Results Obtained in the Walk Test

The numerical results of the RSRP levels obtained in the walk test are presented in Figure 4.2. In the leftmost side of the figure, a graph with measurements of the RSRP level of the walk test is represented

in terms of the Cumulative Distribution Function (CDF) and, by the right side a table, where some of those values are depicted. The graph represents the RSRP Level using dBm in the horizontal axis and the CDF using percentages in the vertical axis, as previously mentioned. The highest value of RSRP measured throughout the route was -60.8 dBm. This value was found only once among all the samples and it corresponds to 0.024 % of all the valid measurements. The graph shows that as the RSRP level decreases, more samples are included. Considering a signal level of -70.8 dBm, which corresponds to a step value of -10 dBm when compared to the highest RSRP level, the percentage of samples increases to 2.189 %. As seen in the table, 50 % of the samples have a RSRP level greater than or equal to -90.8 dBm. The lowest value of RSRP level measured during the walk test was -118.9 dBm. Each of these measurements correspond to the strongest signal level received.

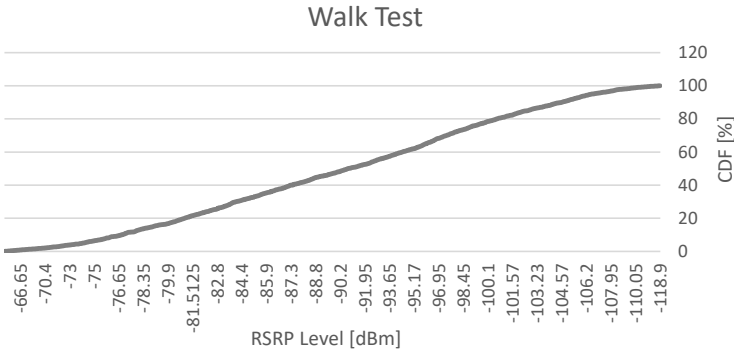

CDF (%)	RSRP Level (dBm)
5	-74.1
10	-76.95
25	-82.55
50	-90.8
75	-98.95
90	-104.6
95	-106.57

Figure 4.2: CDF of the Walk Test RSRP Results

The first prediction with radio models to be presented is in Figure 4.3 and it corresponds to the RSRP obtained with the Okumura-Hata model, using a 2D database. In the figure, the whole polygon area is presented coloured according to the expected RSRP, to allow a better perception of the behaviour of each model. However, the data used to perform the comparisons between the propagation models and the data measured in the walk test is restricted to the coverage predicted for the buffer area only. The scale of all the RSRP coverage predictions is the same as the one used and presented in Figure 4.1 and the histograms are also coloured accordingly.

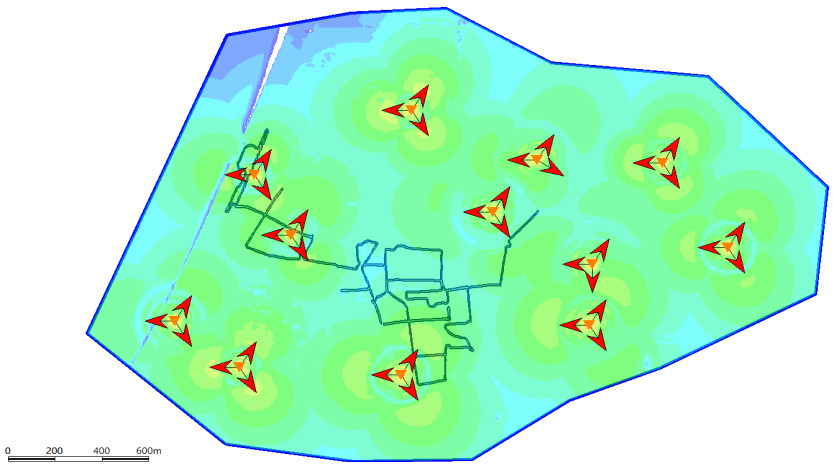

Figure 4.3: RSRP Coverage Predictions of the Okumura-Hata model

In Figure 4.4, a histogram depicts the distribution of the buffer area along with the corresponding predicted RSRP level. Only 0.436 % of the buffer area is expected to have RSRP levels in the range of -70 dBm and -65 dBm, the highest range achieved when using this propagation model. The range of values that is predicted to cover a wider area corresponds to a signal level in the range of -85 dBm to -80 dBm which will cover 30.76 %. Values of RSRP between -90 dBm and -85 dBm are expected to cover around 29.513 % of the buffer area. The whole area would theoretically obtain RSRP levels in the range of -100 dBm and -65 dBm. It is worth to mention that in the walk test 50 % of the samples had RSRP levels greater than or equal to approximately -90 dBm. Whilst running the prediction with the Okumura-Hata model, if we consider a RSRP level greater than or equal to -90 dBm, it attains around 70 % of the buffer area. If we evaluate the simulated RSRP level of 50 % of the buffer area, we conclude it falls in the range of -90 dBm to -85 dBm and it corresponds to -86.7 dBm.

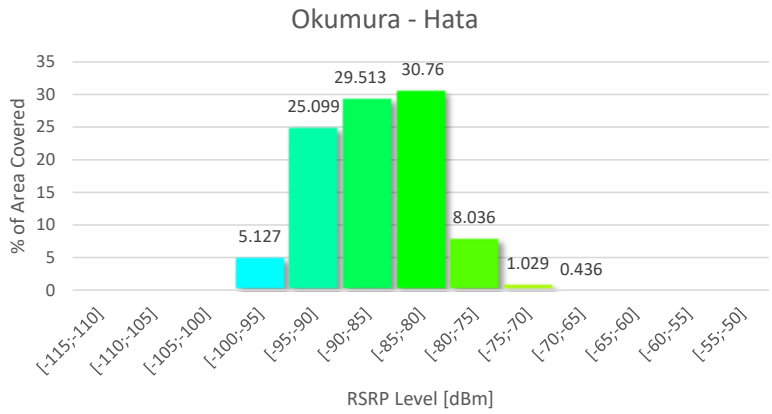

Figure 4.4: Histogram of the RSRP Coverage Predictions of the Okumura-Hata model

The prediction presented in Figure 4.5 was obtained using the COST 231-Hata model. As it can be observed when using this propagation model, RSRP coverage levels are overall lower than compared to Okumura-Hata model. Similarly to the previous case, the whole polygon area is represented although only the buffer area has been considered for comparison purposes and presented in the histograms and CDF plots.

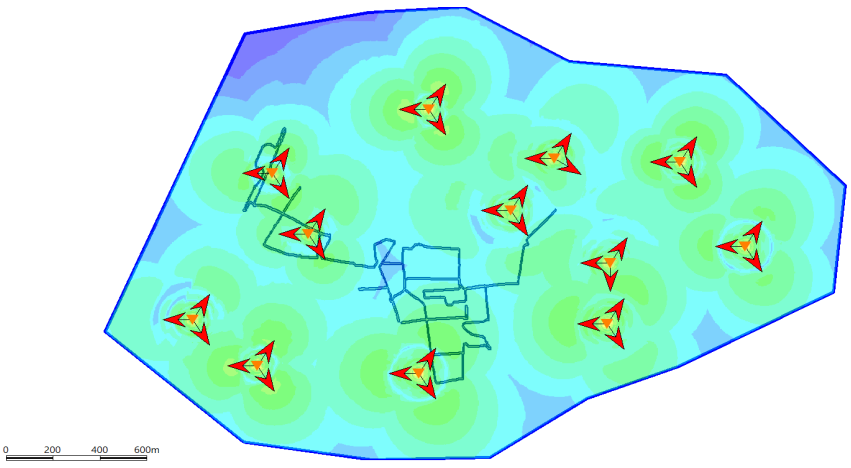

Figure 4.5: RSRP Coverage Predictions of the COST 231-Hata model

The histogram that presents the distribution of the expected RSRP levels in the buffer area using the COST 231-Hata and a 2D database is shown in Figure 4.6. As mentioned, the prediction with this model reveals an overall lower RSRP level. The buffer area is expected to have RSRP levels from -105 dBm to -75 dBm. The higher values of RSRP fall in the category of -80 dBm to -75 dBm and correspond only to 0.99 % of the area. While with the Okumura-Hata model RSRP levels between -85 dBm and -80 dBm covered the highest percentage of area, with the COST 231-Hata the same range of values covers only 8.135 % of the area. The highest percentage of area covered corresponds to 30.899 % and the obtained RSRP levels range from -90 dBm to -85 dBm. These values are close to the ones obtained with the Okumura-Hata model for the same interval of RSRP levels. The lowest range of values corresponds to -105 dBm and -100 dBm which covers 4.691 % of the buffer area. Approximately, 50 % of the buffer area is covered with a RSRP level that reaches -91.7 dBm.

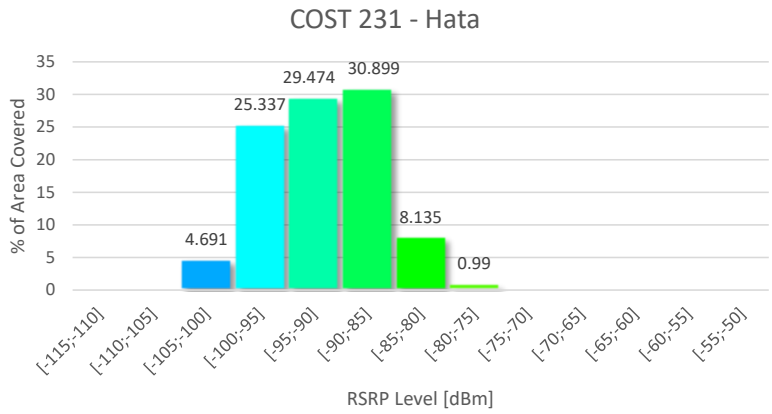

Figure 4.6: Histogram of the RSRP Coverage Predictions of the COST 231-Hata model

The visual representation of the coverage prediction in the polygon area using the SPM and a 2D database can be observed in Figure 4.7. The results of the coverage with this model reveal distinctively higher RSRP levels as one can note by comparing the colour schemes of this coverage and the previously presented coverage predictions.

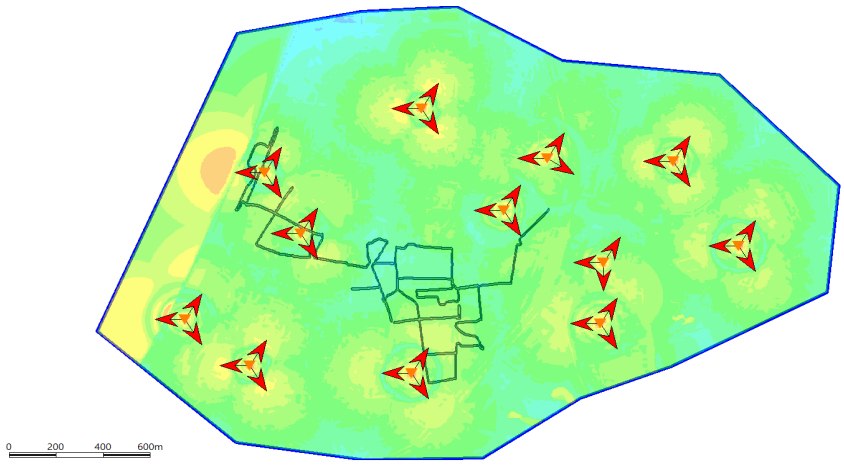

Figure 4.7: RSRP Coverage Predictions of the SPM 2D

The histogram in Figure 4.8 presents the prediction of the values of RSRP obtained in the buffer

area when using the SPM and a 2D database. According to this propagation model, the buffer area has RSRP values ranging from -95 dBm to -60 dBm. The majority of the area has a RSRP level varying between -80 dBm and -75 dBm, over 32.759 % of the area. The same range of values covered only 0.99 % when the predictions were performed with the COST 231-Hata and 8.036 % with the Okumura-Hata. The lowest set of values correspond to values in-between -95 dBm and -90 dBm which cover 1.485 % of the buffer area, which means approximately 98.515 % of the area is covered with RSRP levels above -90 dBm. Considering the cumulative distribution of the area covered, 50 % of the buffer area reached a RSRP level of -80.55 dBm.

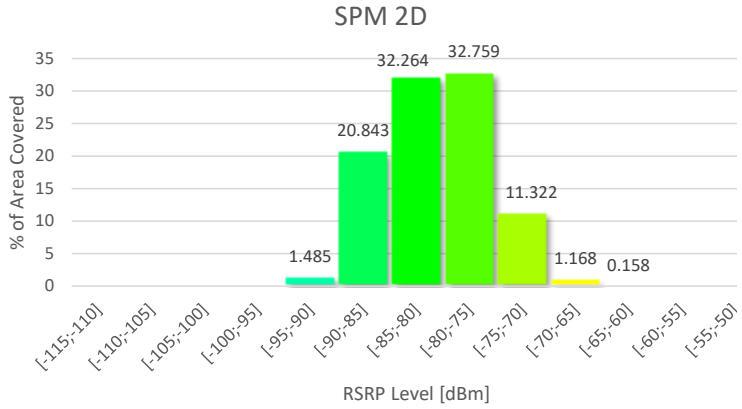

Figure 4.8: Histogram of the RSRP Coverage Predictions of the SPM 2D

The prediction presented in Figure 4.9 uses the SPM and as opposed to the aforesaid predictions a 2.5D database. The use of this type of database leads to a more accurate representation of the environment as now each clutter class has a specific height instead of only having a clutter class with a pre-determined loss value. The higher level of accuracy is visible in the level of detail of the coverage prediction where the streets are discernible from the buildings, which did not happen in the previous predictions.

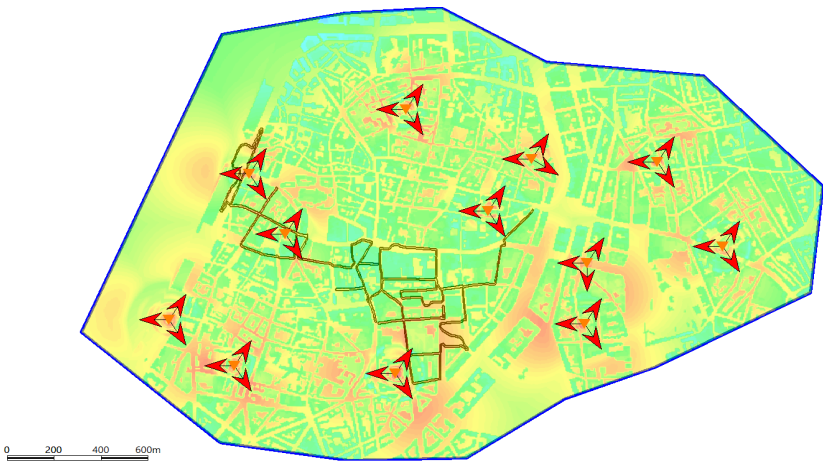

Figure 4.9: RSRP Coverage Predictions of the SPM 2.5D

The histogram with the results of the coverage predictions obtained with 9955 is shown in Figure 4.10. Using the SPM as propagation model and a 2.5D database, less than 12 % of the buffer area is

covered by RSRP levels that range from -95 dBm to -75 dBm whereas when the 2D database was used with the same propagation model the area covered by those same RSRP levels was 87.351 %. The range of RSRP levels of -70 dBm to -65 dBm are the ones that according to the prediction cover a wider area, corresponding to 42.755 % of the total buffer area. About 18.5 % of the area obtained a RSRP level higher than -65 dBm. In this case, 99.426 % of the area has a predicted RSRP level above -90 dBm. Also considering the cumulative distribution of the area covered, 50 % of the buffer area obtained in the simulations a RSRP level of -68.45 dBm.

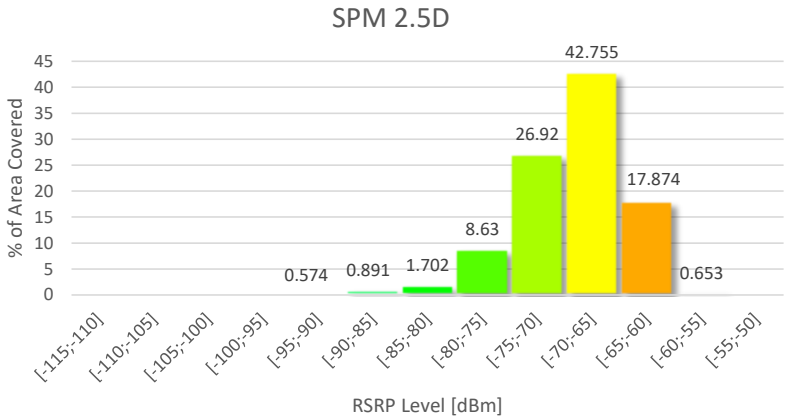

Figure 4.10: Histogram of the RSRP Coverage Predictions of the SPM 2.5D

The RSRP coverage prediction in the polygon area using the WinProp UDP Outdoor model and a 3D database is represented in Figure 4.11. The 3D database, as previously mentioned, differs from a 2.5D database because it includes the height of every single building or obstacle that exist in the area. The 2.5D database only uses a standard height for all the elements that belong to a specific clutter class. The UDP model determines the dominant path between transmitter and receiver using a tree like structure of convex nodes. As such, building vectors were pre-processed. In the outdoor mode, the model considers all the buildings but it does not include the added loss values related to the them.

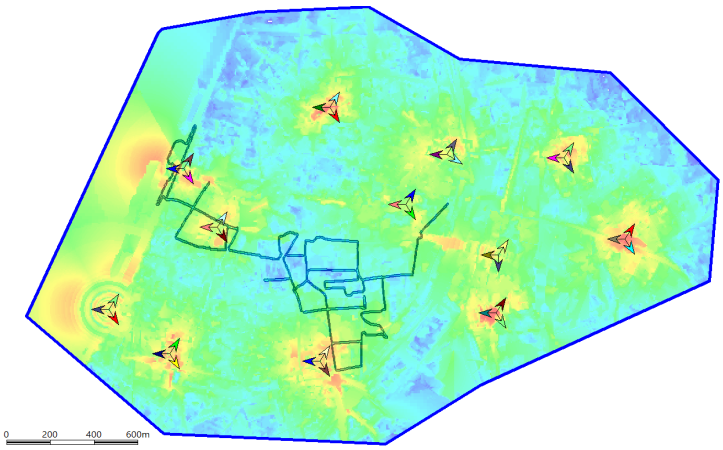

Figure 4.11: RSRP Coverage Predictions of the UDP Outdoor Model

The histogram with the numerical results obtained with the WinProp UDP Outdoor model are shown in Figure 4.12. This model shows a wider range of RSRP levels than previous models. Around 6 % of

the buffer area is covered by RSRP levels that range from -105 dBm to -100 dBm whereas almost 20 % of the area obtained RSRP levels in the range of -100 dBm to -95 dBm. The RSRP levels ranging from -85 dBm to -80 dBm cover a wider area, corresponding to 21.965 % of the total buffer area. About 15.3 % of the area obtained a RSRP level higher than -80 dBm. In this case, 57.947 % of the area has a predicted RSRP level higher than -90 dBm. If we evaluate the simulated RSRP level of 50 % of the buffer area, we conclude it falls in the range of -90 dBm to -85 dBm and it corresponds more precisely to -87.75 dBm.

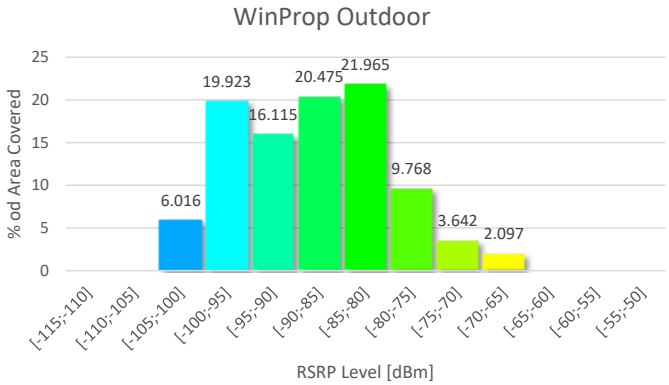

Figure 4.12: Histogram of the RSRP Coverage Predictions of the UDP Outdoor Model

The prediction presented in Figure 4.13 was obtained using the WinProp UDP Indoor as the propagation model and a 3D database. In the indoor mode this model considers all the buildings and its' specific height as before, but it assumes the signal penetrates into the buildings and calculates the signal level indoors. Therefore, the WinProp UDP Indoor model includes an extra loss value corresponding to the buildings materials.

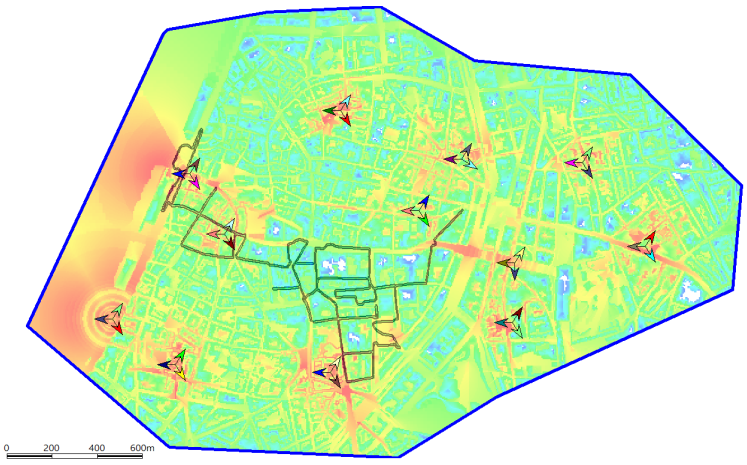

Figure 4.13: RSRP Coverage Predictions of the UDP Indoor Model

The histogram in Figure 4.14 presents the prediction of the values of RSRP obtained in the buffer area when using the WinProp UDP Indoor model. Using this model a wider range of RSRP levels was found in the buffer area. While the majority of the area still obtained values ranged between -100 dBm and -80 dBm, 14.405 % of the area studied obtained a RSRP level higher than -80 dBm. According

to the simulation, around 10.5 % of the buffer area obtained RSRP levels lower than -100 dBm. The prediction results also show that the percentage of area covered by RSRP levels higher than -90 dBm is close to 56 %. Considering the cumulative distribution of the area covered, half of the buffer area reached a RSRP level of -88.55 dBm.

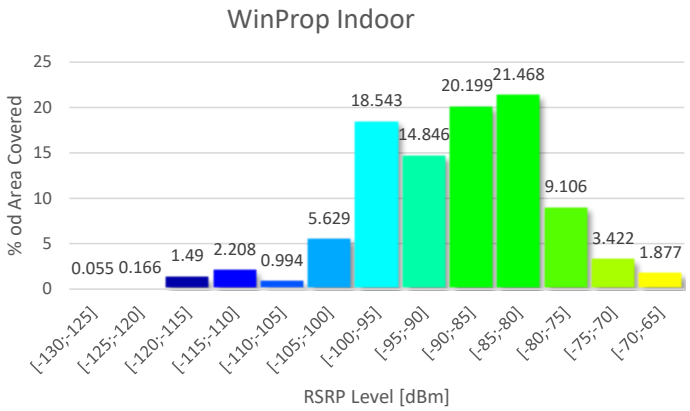

Figure 4.14: Histogram of the RSRP Coverage Predictions of the UDP Indoor Model

In Figure 4.15 a graph comparing the RSRP coverage results of every propagation model is presented. Some of the values of the graph shown in Figure 4.15 are depicted in Table 4.1.

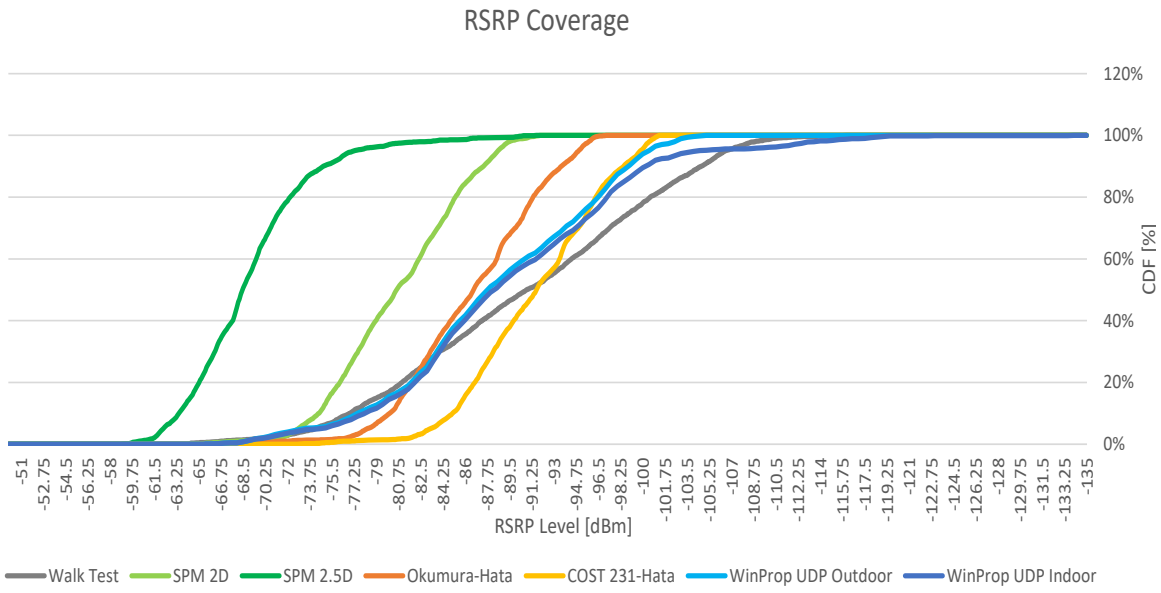

Figure 4.15: Comparison of RSRP Coverage Predictions

The SPM 2.5D appears to be highly optimistic with a CDF curve distant from the curve of the walk test results. The SPM 2.5D simulated values as high as -58.8 dBm while the highest values obtained during the walk test were -60.8 dBm. In comparison the highest value calculated by SPM but with a 2D database was -63.8 dBm. The highest value obtained by the simulation of Okumura-Hata model was -67.7 dBm and with COST 231-Hata was -72.6 dBm. The simulations with WinProp UDP model show that it obtained values more aligned with the measurements retrieved during the walk test. Both WinProp UDP models predicted -65.5 dBm as the highest RSRP level in the buffer area.

Table 4.1: Comparison of CDF Results of RSRP Coverage Predictions

CDF (%)	RSRP Level (dBm)						
	Walk Test	Okumura-Hata	COST 231-Hata	SPM 2D	SPM 2.5D	UDP Outdoor	UDP Indoor
5	-74.1	-78.25	-83.25	-72.8	-62.2	-73.25	-74.5
10	-76.95	-80.05	-85.05	-74.45	-63.45	-77.5	-78.1
25	-82.55	-82.55	-87.55	-76.85	-65.65	-83	-83.4
50	-90.8	-86.7	-91.7	-80.55	-68.45	-87.75	-88.5
75	-98.95	-90.75	-95.7	-84.6	-71.3	-95.25	-96.3
90	-104.6	-93.6	-98.5	-87.45	-74.85	-99	-100.2
95	-106.57	-95	-99.85	-88.6	-77.25	-100.5	-104.25

The results can also be interpreted by separating the results by power level. In the lower range of signal power the WinProp UDP Indoor is the model that reaches a RSRP level closest to the one obtained in the walk test. In this case for a CDF value of 95 % WinProp UDP Indoor obtained -104.25 dBm while the walk test measurements resulted in -106.57 dBm.

As the signal power increases, the WinProp UDP Outdoor and the COST 231-Hata model also tend to approximate more to the walk test results. When the walk test obtained -98.85 dBm for a CDF value of 75 %, the result of the COST 231-Hata model was -95.7 dBm while WinProp UDP achieved -95.25 dBm and -96.3 dBm, for the outdoor and indoor mode respectively. When the signal power increases and crosses the -85 dBm mark, the Okumura-Hata model starts to obtain much better results than the COST 231-Hata model. For a CDF value of 25 % the walk test obtained a RSRP level of -82.55 dBm while Okumura-Hata also attained -82.55 dBm and the COST 231-Hata result was-87.55 dBm. In the higher range of signal power both WinProp UDP models closely align with the walk test results, as well as the SPM 2D until around -72 dBm.

4.1.2 RSRQ Coverage Results

The results of the RSRQ levels obtained in the walk test were also added to 9955 and are represented in Figure 4.16. The scale portrayed in the figure ranges from lower RSRQ values such as -22 dB to higher ones like -6 dB. Although the RSRQ levels measured in the walk test did not reach a value lower than -17.2 dB, the scale includes some lower values to account for the results obtained in the predictions of the different models.

The results of the RSRQ levels obtained in the walk test are presented in Figure 4.17. As seen in the graph, by the left, the results are presented using the CDF in the vertical axis and the RSRQ level measured in dB in the horizontal axis. The graph shows that the highest value of RSRQ measured throughout the route was -6 dB, which corresponds to 0.253 % of all the values obtained. By observing the table one concludes that 50 % of the samples have a RSRQ level greater than or equal to -8.95 dB. The lowest value of RSRQ level measured during the walk test was -17.2 dB. Approximately 98 % of the samples have a RSRQ level equal to or greater than -15 dB. Each of these measurements correspond

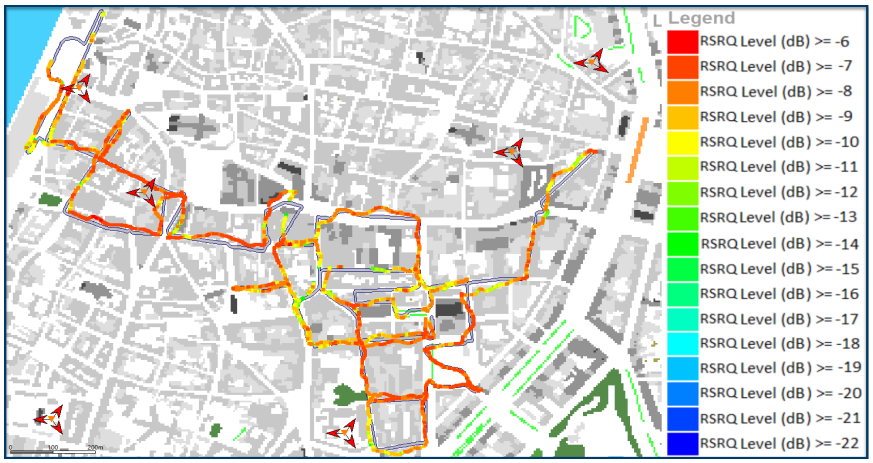

Figure 4.16: RSRQ Results Obtained in the Walk Test

to the signal received by the best server at that moment and exact location.

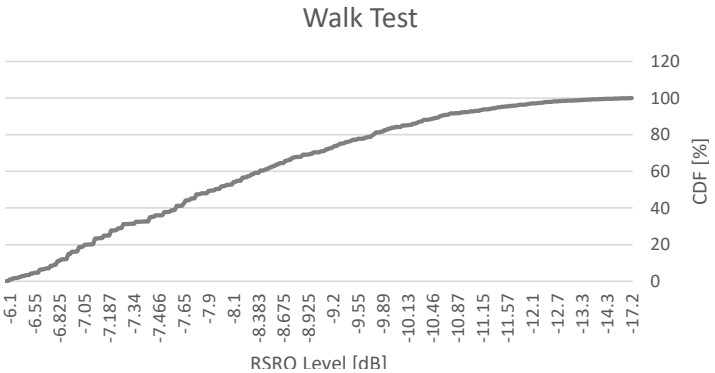

CDF (%)	RSRQ Level (dB)
5	-6.575
10	-6.79
25	-7.175
50	-7.95
75	-9.35
90	-10.6
95	-11.47

Figure 4.17: CDF of the Walk Test RSRQ Results

The results of the coverage predictions for the RSRQ levels obtained by the different models are only presented in the form of a histogram as the results are quite similar visually and the differences cannot be perceived easily.

The histogram with the distribution of the expected RSRQ levels in the buffer area using the Okumura-Hata model and a 2D database is presented in Figure 4.18. The whole area obtained RSRQ values between -20 dB and -13 dB. As depicted, 30.245 % of the area obtained RSRQ levels between -14 dB and -13 dB. According to the prediction the lower step of values only covers 1.03 % of the buffer area, while values located in -19 dB and -18 dB cover 5.344 % of the area. The percentage of area that obtained a signal level higher than -15 dB corresponds to 53.34 %. When assessing the cumulative distribution of the RSRQ levels obtained with Okumura-Hata, we conclude that for 50 % of the buffer area it reaches -16.85 dB.

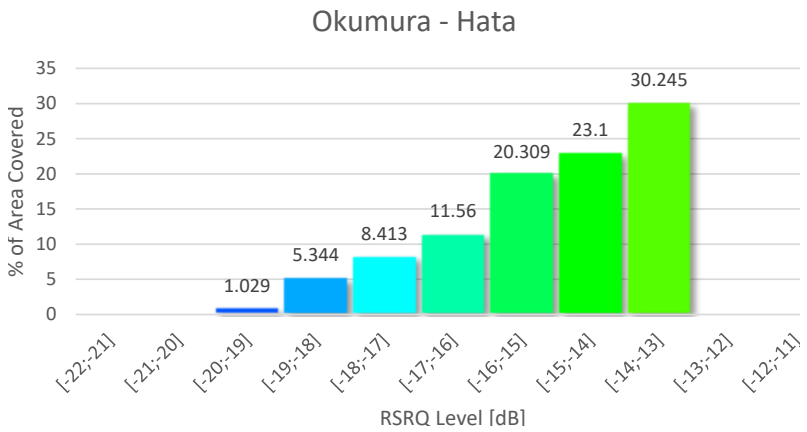

Figure 4.18: Histogram of the RSRQ Coverage Predictions of the Okumura-Hata model

In Figure 4.19, a histogram depicts the distribution of the buffer area along with the corresponding predicted RSRQ level, using the COST 231-Hata as the propagation model and a 2D database. Similarly to the prediction with Okumura-Hata, the RSRQ values range from -20 dB to -13 dB. The main differences are in the range of values from -20 dB and -19 dB that now cover 1.92 % of the buffer area whilst the previous model only covered 1.03 % of the area. The percentage of area covered by values from -14 dB to -13 dB also suffered a slight change, decreasing to 29.77 %. According to the histogram 52.85 % of the area has RSRQ values higher than -15 dB while in the walk test the same RSRQ levels included 98 % of the samples. Considering the cumulative distribution of the area covered, half of the buffer area reached a RSRQ level of -14.85 dB.

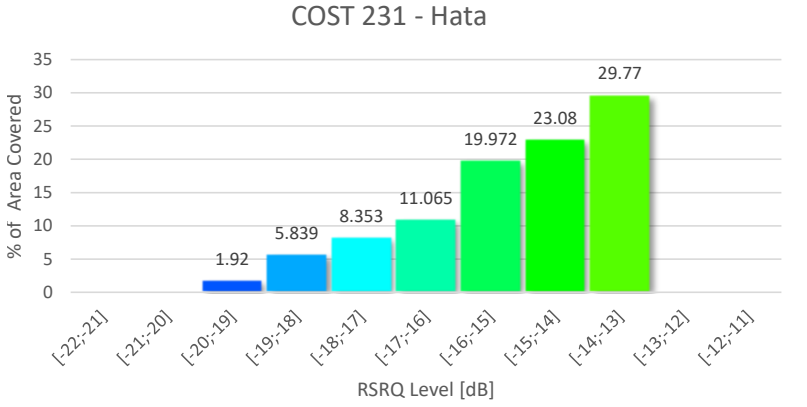

Figure 4.19: Histogram of the RSRQ Coverage Predictions of the COST 231-Hata model

The histogram with the results of the coverage predictions obtained with the SPM as the propagation model and a 2D database is shown in Figure 4.20. The RSRQ values predicted now range from -21 dB to -13 dB. However, the contribution of the values of RSRQ lower than -20 dB is minimal only contributing to cover 0.04 % of the buffer area. In this case, 50 % of the area is covered by a RSRQ level of approximately -15 dB.

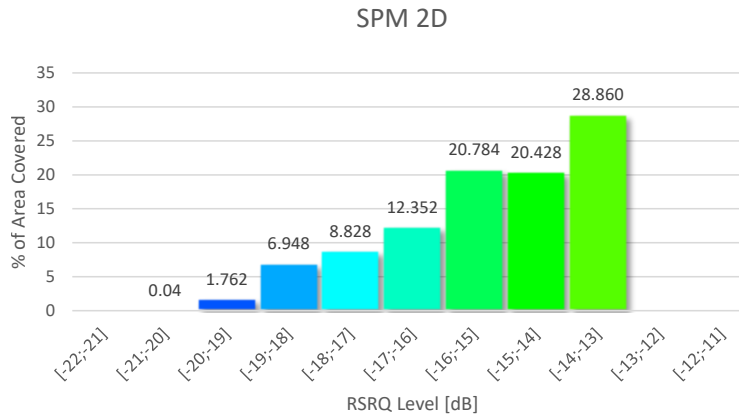

Figure 4.20: Histogram of the RSRQ Coverage Predictions of the SPM 2D

The results of the RSRQ level predictions with the SPM and a 2.5D database are represented in Figure 4.21. Less than 14 % of the buffer area is covered by RSRQ levels in the range of -22 dB and -18 dB. The prediction results of the SPM with the 2D database showed that only 21.1 % of the area was covered with RSRQ levels of -18 dB to -16 dB. In this case, with the same propagation model but using the 2.5D database the same set of values cover 28.4 % of the buffer area. The set of values covering a wider area corresponds to values set between -16 dB and -15 dB which cover 24.03 % of the buffer area. Signal levels higher than -15 dB cover a total area of 34.2 %. If we evaluate the simulated RSRQ level of 50 % of the buffer area, we conclude it falls in the range of -16 dB to -15 dB and it corresponds to -15.6 dB.

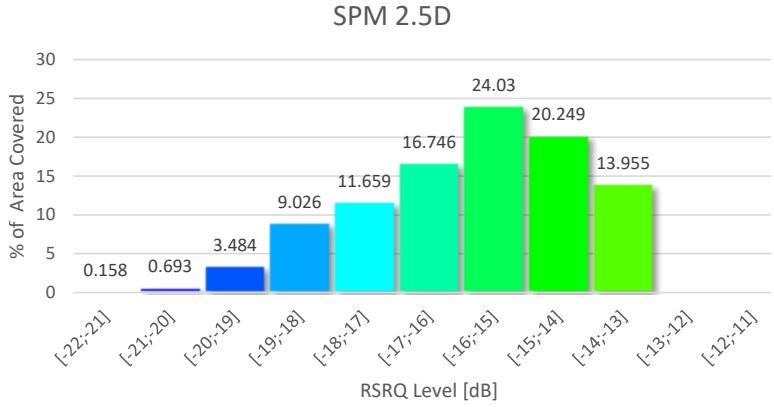

Figure 4.21: Histogram of the RSRQ Coverage Predictions of the SPM 2.5D

The histogram with the results of the coverage predictions obtained with WinProp UDP Outdoor as the propagation model and a 3D database is shown in Figure 4.22. The RSRQ values predicted range from -20 dB to -11 dB, reaching higher values than previous predictions. The prediction results also show that the percentage of area covered by RSRQ levels higher than -15 dB is 78.808 %. Considering the cumulative distribution of the simulated RSRQ levels, 50 % of the buffer area attained a RSRQ level of -13.75 dB with WinProp UDP Outdoor.

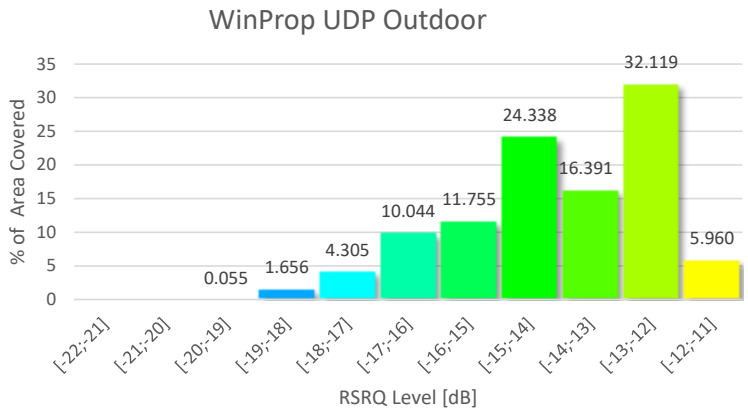

Figure 4.22: Histogram of the RSRQ Coverage Predictions of the WinProp UDP Outdoor model

The histogram with the distribution of the expected RSRQ levels in the buffer area using the WinProp UDP Indoor and a 3D database is presented in Figure 4.23. The whole area obtained RSRQ values between -22 dB and -11 dB. However, the contribution of RSRQ values lower than -19 dB is minimal and only contributes to cover 0.276 % of the buffer area. The results are similar to the ones obtained with WinProp UDP in the Outdoor mode. However, the percentage of area that obtained a signal level higher than -15 dB corresponds to 71.745 %. Also, for reference, with a CDF value of 50 % this model obtained RSRQ levels of -13.8 dB.

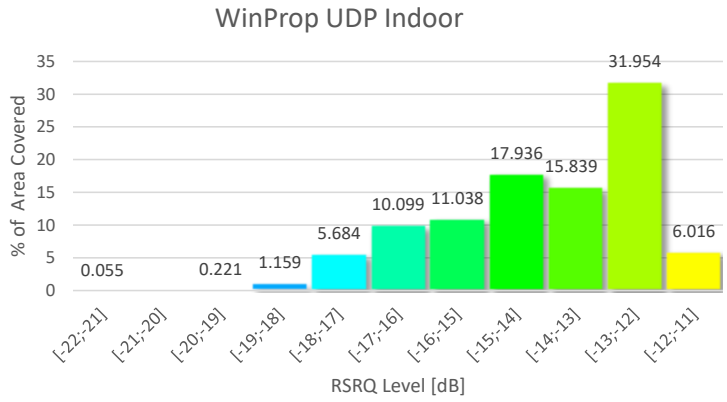

Figure 4.23: Histogram of the RSRQ Coverage Predictions of the WinProp UDP Indoor model

In order to compare the RSRQ results obtained by every model, a graph with the cumulative distribution function of the results is shown in Figure 4.24. Some values of the graph of Figure 4.24 are depicted in Table 4.2.

As opposed to the RSRP results, none of the models used for the RSRQ coverage prediction immediately stands out as the best fit, seeing as the walk test clearly obtained results with a higher RSRQ level. The walk test measurements of the RSRQ range from -17.2 dB to -5.8 dB. The model that obtains a highest value of RSRQ is the WinProp UDP with -11.5 dB for both the indoor and the outdoor mode. With the other 4 models the highest value of RSRQ is around -13 dB.

In the coverage by area analysis, the samples obtained in the walk test are compared to a coverage

area and not individual points. In order to reduce the error both measured and predicted results are presented in terms of a cumulative distribution. However, in the RSRQ results the number of individual samples is much lower than in the RSRP case, which can contribute to the general behaviour found in Figure 4.24.

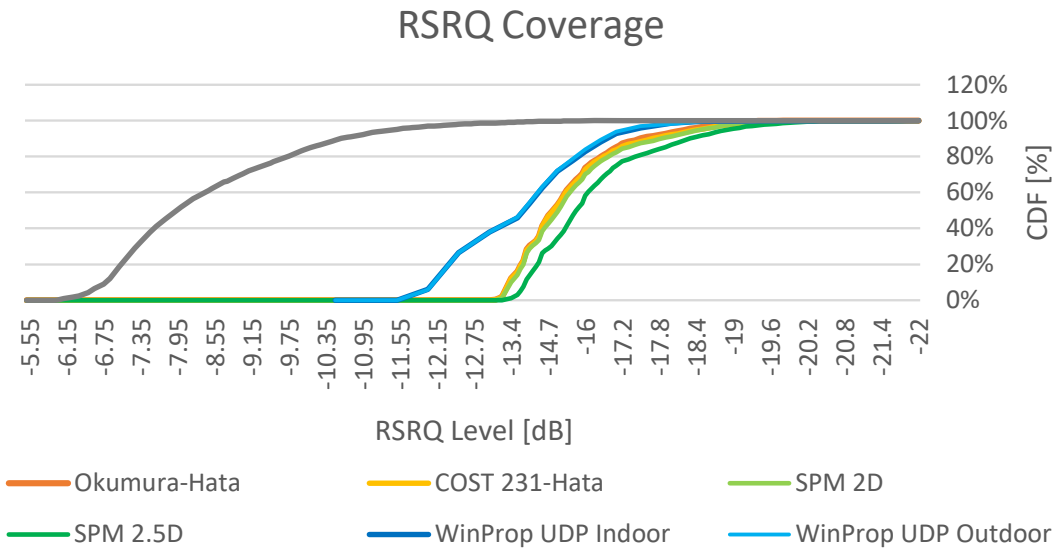

Figure 4.24: Comparison of RSRQ Coverage Predictions

Table 4.2: Comparison of CDF Results of RSRQ Coverage Predictions

CDF (%)	RSRQ Level (dB)						
	Walk Test	Okumura-Hata	COST 231-Hata	SPM 2D	SPM 2.5D	UDP Outdoor	UDP Indoor
5	-6.575	-13.25	13.25	13.3	-13.6	-11.9	-11.95
10	-6.79	-13.35	-13.35	-13.4	-13.85	-12.2	-12.3
25	-7.175	-13.8	-13.8	-13.85	-14.45	-12.45	-12.5
50	-8.95	-16.85	-14.85	-15	-15.6	-13.75	-13.8
75	-9.35	-16.05	-16.15	-16.35	-17	-15.3	-15.2
90	-10.60	-17.4	-17.7	-17.85	-18.25	-16.5	-16.75
95	-11.47	-18.25	-18.45	-18.45	-18.9	-17.25	-17.48

4.2 Point-to-Point Results

The comparison by coverage area might not be the most appropriate considering the samples obtained in the walk test are compared to a coverage area and not individual points. In order to be as accurate as possible and present a fair comparison of predictions against walk test results, a point to point analysis has been made.

As already stated, some walk test samples were found to be misplaced. Therefore, all indoor locations were moved to the nearest possible outdoor location for the sake of comparison against the

propagation models. The simulations later used that new location to retrieve the equivalent RSRP or RSRQ level. The point-to-point RSRP comparison of Okumura-Hata model and the walk test results can be observed in Figure 4.25. The total number of valid samples obtained from this simulation that correspond to the locations of the walk test is 4093. The total number of samples of the walk test corresponds to 4203. This difference comes from points where the simulation tool was not able to attribute a RSRP value due to resolution constraints.

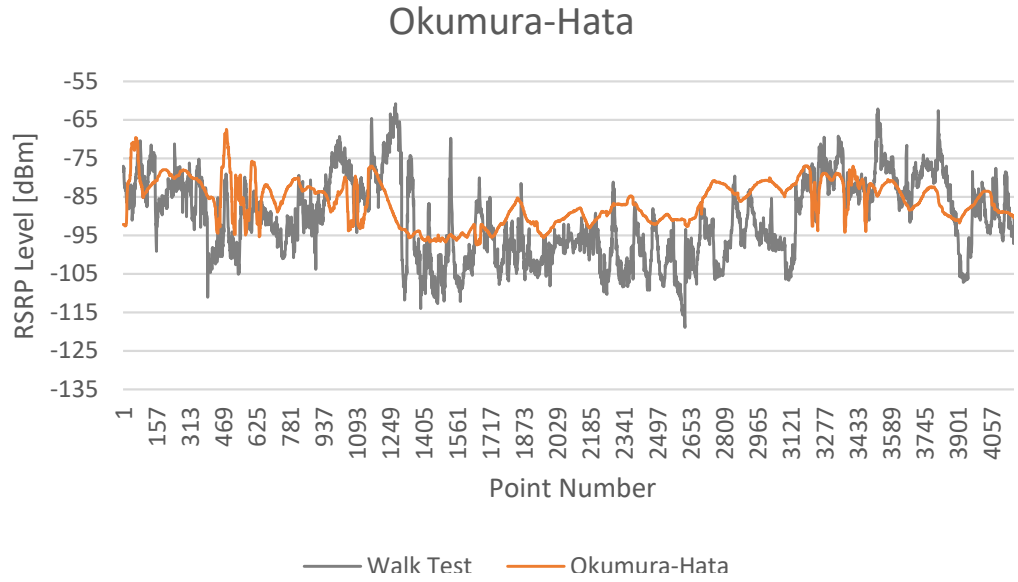

Figure 4.25: Point-to-Point Comparison of Okumura-Hata model and Walk Test RSRP Results

The RSRP values predicted with COST 231-Hata model are depicted alongside with the equivalent values measured during the walk test in Figure 4.26. The total number of valid samples obtained from the prediction with this model was 3868. The results appear to be similar to the ones obtained with Okumura-Hata model although less points were obtained in this prediction.

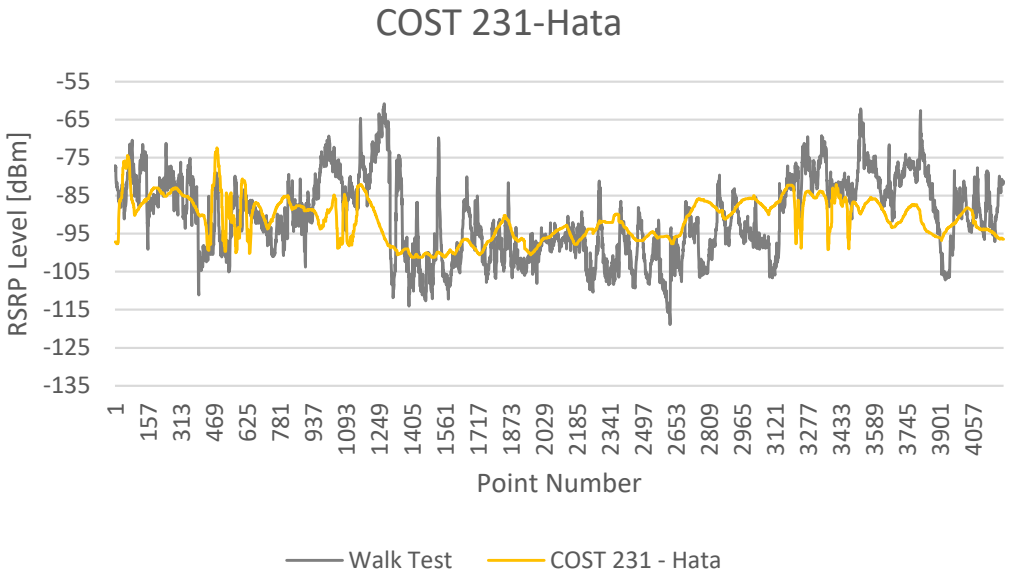

Figure 4.26: Point-to-Point Comparison of COST 231-Hata model and Walk Test RSRP Results

The point-to-point comparison of measured results and values obtained by simulating the SPM with a 2D database are presented in Figure 4.27. The total number of valid samples obtained with SPM 2D was 4131. The results of this model differ from the previous ones. The simulation of SPM using a 2D database obtained higher RSRP levels than the ones measured. As such, this model can be considered optimistic.

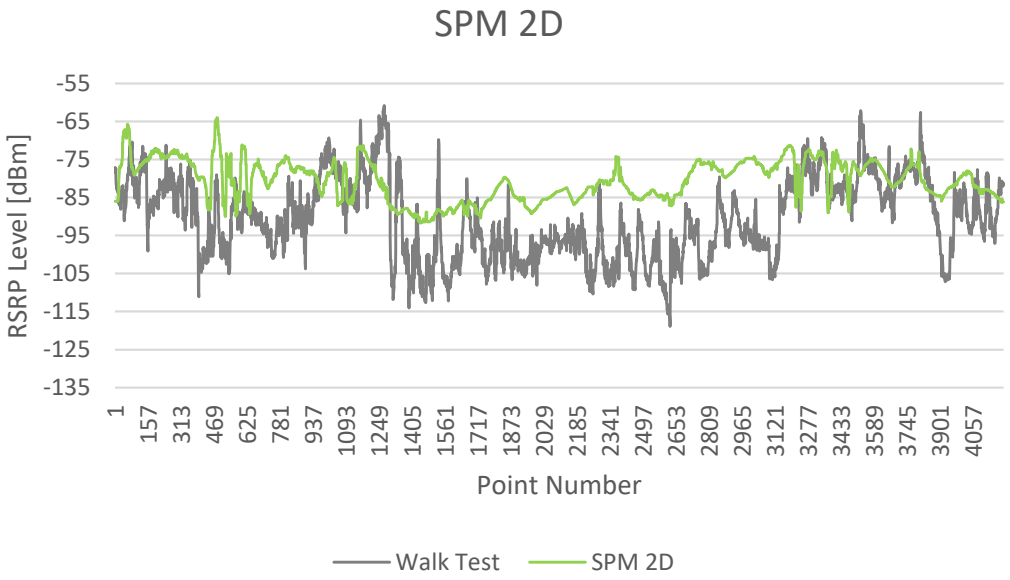

Figure 4.27: Point-to-Point Comparison of SPM 2D and Walk Test RSRP Results

The simulated results obtained with SPM and a 2.5D database are placed with the measured values in Figure 4.28. The total number of valid samples obtained with SPM 2.5D was 4121. This model is even more optimistic than the previous one, as overall it obtained results 15 dB higher than the actual measured results.

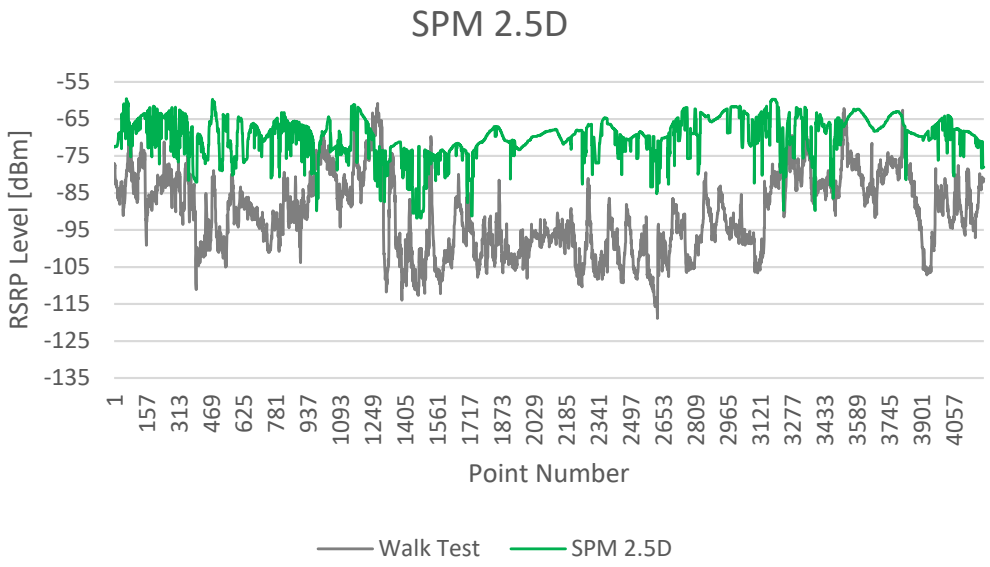

Figure 4.28: Point-to-Point Comparison of SPM 2.5D and Walk Test RSRP Results

The point-to-point results of the simulation with WinProp UDP Outdoor are presented in Figure 4.29. The total number of valid samples obtained in this simulation was 4160. According to the plots, the predicted results of this model are overall more aligned with the measured results. The WinProp UDP Outdoor model obtains RSRP results much closer to the measurements of the walk test than any previous predictions.

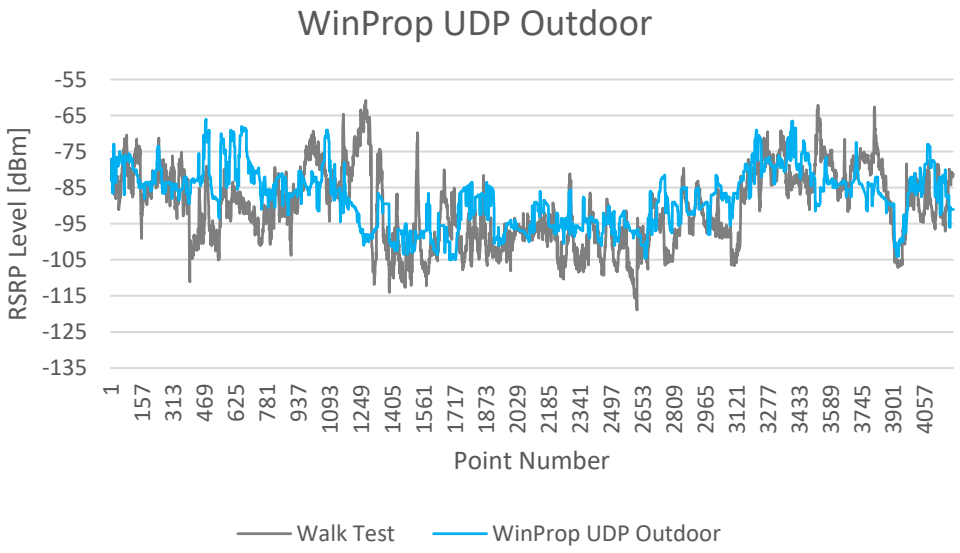

Figure 4.29: Point-to-Point Comparison of WinProp UDP Outdoor model and Walk Test RSRP Results

The final results of the simulation with WinProp UDP Indoor model are presented in Figure 4.30. The total number of samples was 4157. Although the results of the WinProp UDP Indoor do not appear to be quite as aligned with the results of the walk test as the WinProp UDP Outdoor, the results are still quite coherent.

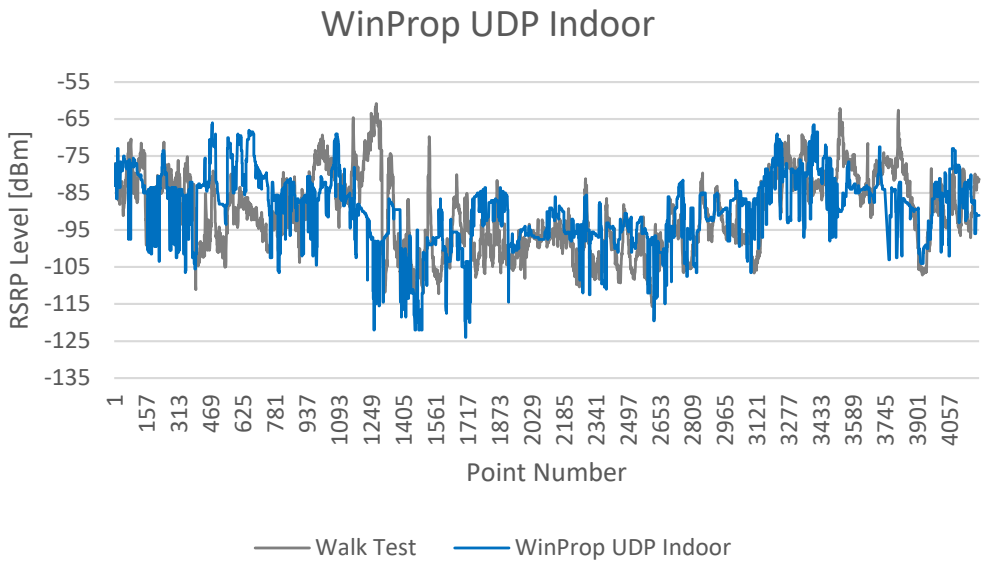

Figure 4.30: Point-to-Point Comparison of WinProp UDP Indoor model and Walk Test RSRP Results

The point-to-point comparison of the RSRQ results will not be presented graphically as the results

are too similar amongst them. However, the data will be included in the statistical analysis performed in the following section.

4.3 Validation of Results

A statistical analysis of the accuracy of each model studied is necessary. The following statistical performance metrics were used: Mean Absolute Error (MAE) and Standard Deviation (SD). These metrics were calculated in linear units and converted back to dB.

$$MAE = \frac{1}{N}\sum_{i=1}^{N}|S_i^M - S_i^P| \tag{4.1}$$

$$SD = \sqrt{\frac{1}{N}\sum_{i=1}^{N}(|S_i^M - S_i^P| - \mu)^2} \tag{4.2}$$

where μ is the absolute error.

4.3.1 Analysis of RSRP Results

The total number of samples retrieved during the walk test used in this study was 4203. The MAE and SD of the RSRP point-to-point results are presented in Table 4.3. Also stated in the table is the number of valid samples obtained in the point-to-point analysis of each propagation model. According to the results in the table the propagation model that obtains the best approximation to the walk test is Okumura-Hata model with a MAE of 13.533 dB. It is followed closely by COST 231-Hata with a MAE of 14.190 dB and WinProp UDP Outdoor with 15.621 dB.

Table 4.3: Statistical Analysis of RSRP Results

Model	Samples	MAE (dB)	SD (dB)
Okumura – Hata	4093	13.533	17.333
COST 231 – Hata	3868	14.190	21.188
SPM 2D	4131	17.953	21.507
SPM 2.5D	4121	29.213	33.087
WinProp UDP Outdoor	4160	15.621	24.086
WinProp UDP Indoor	4157	26.466	38.950

In Table 4.4, the statistical analysis of the RSRP results is performed but with a variation. In this case, the samples that had an absolute error higher than or equal to 30 dB were excluded. This analysis attempts to reduce the effect of the outliers on the overall results. According to these results, the model that obtained the lowest MAE is now the WinProp UDP Outdoor with 12.427 dB. Although COST 231-Hata and Okumura-Hata still achieved a MAE of 12.659 dB and 13.486 dB, respectively, the main difference lays in the result of WinProp UDP Indoor. This model now obtained a MAE of 13.712 dB, as

opposed to the inital value of 26.466 dB found in Table 4.3.

Table 4.4: Statistical Analysis of RSRP Results excluding samples with an AE higher than 30 dB

Model	Samples	MAE (dB)	SD (dB)
Okumura – Hata	4092	13.486	17.149
COST 231 – Hata	3848	12.659	17.958
SPM 2D	4117	17.660	20.877
SPM 2.5D	3292	22.833	23.866
WinProp UDP Outdoor	4113	12.427	17.519
WinProp UDP Indoor	4123	13.712	18.553

The results were also divided according to power level in order to better analyse the general behaviour and possible pattern of each model. The results of that analysis can be found in Table 4.5.

Table 4.5: Statistical Analysis of RSRP Results according to Power Level

Model	Walk Test Samples $\leq$ - 85 dBm			Walk Test Samples $>$ - 85 dBm		
	Samples	MAE (dB)	SD (dB)	Samples	MAE (dB)	SD (dB)
Okumura – Hata	2752	13.800	16.584	1341	12.927	18.346
COST 231 – Hata	2552	9.182	11.280	1316	17.858	23.433
SPM 2D	2774	19.522	22.195	1357	8.384	11.104
SPM 2.5D	2784	30.867	33.769	1337	14.606	15.636
WinProp UDP Outdoor	2823	11.955	15.338	1372	18.942	26.439
WinProp UDP Indoor	2820	11.031	16.534	1337	31.270	41.399

By the righthand side the analysis of the walk test samples with a RSRP value lower than or equal to -85 dBm and by the lefthand side the analysis of only the samples higher than -85 dBm.

Okumura-Hata had in both situations a MAE error close to the total MAE shown in Table 4.3. The Okumura-Hata model seems to adapt well to both scenarios. The COST 231-Hata model obtained 9.182 dB of MAE in the lower power scenario and 17.858 dB in the higher power one.

SPM 2D had an opposite behaviour when compared to the COST 231-Hata model. It behaves clearly better in scenarios with higher power RSRP levels. Its MAE was 8.384 dB for that scenario, as opposed to 19.522 dB in the lower power situation.

The SPM 2.5D model followed the pattern of SPM 2D. It achieved a lower MAE in high power scenarios of 14.606 dB and a higher MAE of 30.867 dB when the samples used were below -85 dBm.

WinProp UDP Outdoor presented a lower MAE in the low power scenario, 11.955 dB, than in the general case where it was 15.621, demonstrating that in this case the model is more indicated for lower powers.

The WinProp UDP Indoor model much like the Outdoor version suffered a considerable difference in the MAE. In the general case, first shown in Table 4.3 the MAE was 26.466 dB. For the lower power scenario the MAE calculated for this model was 11.031 dB and for the higher power scenario it was

31.270 dB.

The propagation model that achieved an overall lower MAE in the lower power scenario was COST 231-Hata with a MAE of 9.182 dB. It is worth mentioning that WinProp UDP Indoor had a clear improvement of its error. In the low power scenario its MAE was 11.031 dB whereas in the general analysis its MAE was 26.466 dB. For the higher power signal scenario, the model that achieved the lowest MAE was SPM 2D with 8.384 dB.

In Figure 4.31 the cumulative distribution of the MAE regarding the RSRP results of each model is presented. This plot shows that besides the SPM 2D and SPM 2.5D, the MAE of the other models is more or less contained and is similar amongst each other.

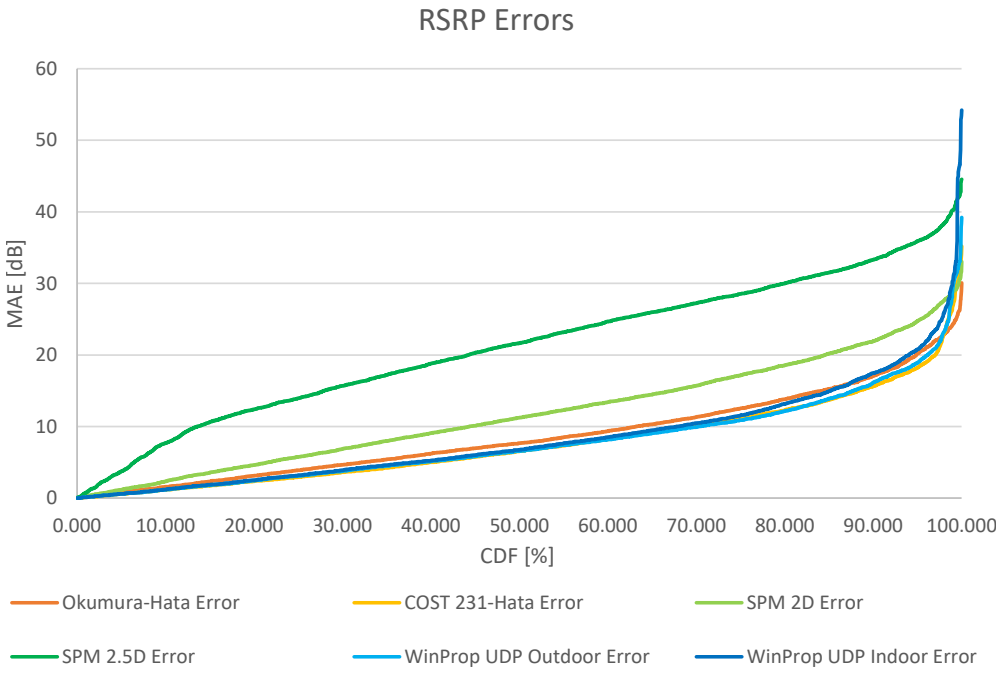

Figure 4.31: Error Comparison of RSRP Results

4.3.2 Analysis of RSRQ Results

The statistical analysis of the point-to-point RSRQ results are shown in Table 4.6. The number of samples used in the simulation of each model, as well as the MAE and SD are presented.

According to these results, the propagation model that obtains the lowest MAE is WinProp UDP Indoor with 6.319 dB. In this comparison however, the difference between the MAE of each model is much lower than in the RSRP case. The model that obtained the highest MAE was SPM 2.5D with 8.127 dB, which is a difference of only 1.808 dB.

In Table 4.7, the statistical analysis of the RSRQ results is performed but with a variation. In this case, the samples that had an absolute error higher than or equal to 10 dB were excluded.

Considering the MAE was already low and stabilized around 7 dB, this variation only contributed to lowering the overall results of the metrics. However, the model that attained the lowest MAE was now the

Table 4.6: Statistical Analysis of RSRQ Results

Model	Samples	MAE (dB)	SD (dB)
Okumura – Hata	4162	7.343	4.733
COST 231 – Hata	4133	7.406	4.859
SPM 2D	3989	7.573	5.052
SPM 2.5D	4155	8.127	5.700
WinProp UDP Outdoor	3645	6.319	3.634
WinProp UDP Indoor	3668	6.326	3.594

Table 4.7: Statistical Analysis of RSRQ Results excluding samples with an AE higher than 10 dB

Model	Samples	MAE (dB)	SD (dB)
Okumura – Hata	3826	6.752	2.486
COST 231 – Hata	3774	6.776	2.552
SPM 2D	3496	6.863	2.643
SPM 2.5D	3534	7.181	2.761
WinProp UDP Outdoor	3549	6.085	3.662
WinProp UDP Indoor	3562	6.082	2.652

WinProp UDP Indoor. The difference between the MAE of the WinProp UDP Outdoor and the WinProp UDP Indoor is minimal consisting of 0.003 dB.

The RSRQ results were also divided according to power level in order to better analyse the general behaviour of each model. The results of that analysis can be found in Table 4.8.

Table 4.8: Statistical Analysis of RSRQ Results according to Power Level

Model	Walk Test Samples $\leq$ - 8 dB			Walk Test Samples $>$ - 8 dB		
	Samples	MAE (dB)	SD (dB)	Samples	MAE (dB)	SD (dB)
Okumura – Hata	1998	6.220	2.970	2164	8.172	5.141
COST 231 – Hata	1975	6.304	3.229	2158	8.217	5.252
SPM 2D	1920	6.421	3.326	1978	8.459	5.450
SPM 2.5D	1985	6.969	4.030	2170	8.969	6.091
WinProp UDP Outdoor	1874	5.292	2.284	1771	7.192	3.952
WinProp UDP Indoor	1889	5.328	2.383	1779	7.183	3.857

On the lefthand side an analysis of the RSRQ point-to-point error is performed for walk test samples below -8 dB. While on the righthand side the same analysis was performed but for higher RSRQ levels. The WinProp UDP Outdoor is the model that obtained the lowest MAE in the lower range signal scenario with a value of 5.292 dB. For the scenario with signal levels with higher values the WinProp UDP Indoor obtained the lowest MAE with a value of 7.183 dB.

The cumulative distribution of the MAE of the RSRQ results of each of the models simulated are

represented in Figure 4.32. According to the plot both simulations performed with WinProp UDP obtain the lowest MAE. The simulation with WinProp UDP Outdoor appears to have fewer outliers as it reaches a lower peak value.

Figure 4.32: Error Comparison of RSRQ Results

Chapter 5

Conclusions

In this chapter, a summary of all the work carried out under the scope of this thesis is provided. Then, some important conclusions are highlighted and to finalize some ideas for future work are discussed.

5.1 Summary

The main goal of this thesis was the study and comparison of propagation models and types of geographic databases that are used in the deployment of small-cells. Several propagation models were simulated in a network planning tool using different types of databases. The results were then compared to actual measurements obtained during a walk test.

In Chapter 2, the fundamental concepts of the relevant technologies to this thesis are presented along with the state of the art. The first section of the chapter is dedicated to LTE. The overall network architecture is described and some of the main features of the radio interface are addressed like the multiple access technique. Regarding the network architecture, the functioning of the network and the fundamental elements that take place in it are described. The second section introduces small-cells and its integration with LTE. Some references are made to important topics such as interference and mobility. Also, particular relevance is given to propagation models and geographical databases. The different types of propagation models are introduced: deterministic, semi-empirical and empirical. Some models are described in detail as they have been tested later on. The distinction between the different types of databases is also presented. The final section includes the state of the art, where studies from the current literature related to small-cells and propagation models are analysed and described.

In Chapter 3, the methodology used in this thesis is explained. Initially, some context is given to understand the general scope of the project. Then, the propagation models tested are described in more detail. In addition, the methods used by the network planning tool, 9955 RNP, to compute the necessary information from each of the different databases are explained. For a 2D database, the information related to the clutter classes is used, in addition to the DTM file which already includes the terrain topography. Each location in the database belongs to a specific clutter class such as open area, urban or dense urban. Each clutter class has an associated loss value used in path loss calculations.

A 2.5D database functions similarly to the 2D but includes an average height per clutter class. The 3D database contains a detailed description of the height and orientation of every structure in the area. The final section of the chapter presents some corrections that were performed to reduce inconsistencies in the measured data. The method used to create the buffer area is also explained. This buffer attempts to limit the coverage predictions to the area where the walk test took place.

Chapter 4 presents the results obtained in this thesis according to the different analysis. The first section presents the results of the coverage by area of the RSRP and the RSRQ. First, the results of the coverage predictions are presented in a histogram for each of the models simulated. Then, a graph with the CDF of all the models is presented to allow a comparison. The model that more closely aligns to the walk test results is the WinProp UDP Outdoor. The following section of this chapter presents the results of the point-to-point comparison for the RSRP. Finally, the last section introduces the statistical analysis of the point-to-point comparisons of the RSRP and the RSRQ. The MAE and SD were calculated for each of the models. Three different analysis were performed. In the first one, every sample was included in the study. This led to conclude that the model with the lowest MAE was Okumura-Hata. In the second analysis, the samples with a high absolute error were excluded to reduce the effect of outliers. According to this analysis the model that obtained the lowest MAE was WinProp UDP Outdoor. The final case analysed the results according to range. The walk test samples were separated into higher or lower than a specific value to test the performance of each model as the distance to the station varied.

Initially, the work proposed in this thesis aspired to compare the results of the same propagation model using different types of databases and different propagation models using the same type of geographical databases. However, the analysis of several propagation models was found to be more difficult than expected. Some propagation models have strict requirements of databases and therefore comparison of the propagation models by themselves was not possible, without also having to take into account the effect of different types of geographical databases. In that sense, they have always been compared as a combination of propagation model and geographical database.

The validity of the walk test is another factor to be taken into consideration. There are several possible sources of errors. Apart from the mobile terminal error (which depending on the vendor might be up to 3 dB), positioning also suffers from inconsistencies, which added another error factor by requiring artificial correction of measurements that had their GPS locations registered indoor when it is known all walk tests were outdoor. Also, it is important to note that the database of the sites' location is prone to errors, since the exact location of the antennas is most of the time unknown and assumed to be the geographical location given for the site. Not only the location of sites and antennas are susceptible to errors but also the exact HW configuration of a given site or cell might be inaccurate by relying on manual input to capture all the relevant radio parameters that have direct impact on the radio propagation. Such parameters include, for example, exact azimuths for sector orientation, mechanical and electrical tilting. Unfortunately, even during the execution of commercial projects, these sources of inaccuracies and errors are frequent and require an engineer with deep understanding of the project environment to obtain the most likely configuration to be found in every site, which ultimately will minimise the errors but not eliminate them completely.

Moving into the analysis of the actual results, a first outlook showed Okumura-Hata and COST 231-Hata obtained the lowest values of MAE, which is somehow surprising considering that these propagation models are the most generic ones. Okumura-Hata obtained a MAE of 13.533 dB, while COST 231-Hata obtained 14.190 dB of MAE. Both models are non-deterministic and based on the Okumura model. This model was developed during the mid 1960's using the data collected in the city of Tokyo, Japan. As such, these models are ideal for urban cities with many low buildings. Antwerp, as it happens, falls particularly well into this scenario, especially in the city centre. The city's architecture is very regular with perpendicular streets and most buildings of similar height, particularly in the area where the walk test took place. The good performance of these models can partly be justified by these factors. In addition, these measurements were performed outdoor and at ground level which corresponds to the conditions these models are applied.

However, in what Okumura-Hata concerns, the validity of results might be questionable due to the absolute radio frequency channel the tested network is operating in, which falls slightly outside the domain of validity of Okumura-Hata, set to 1500MHz, while Antwerp's LTE network operates at 1800MHz.

Still regarding RSRP, going into more detail, it was decided to avoid samples with an absolute error higher than 30 dB and those samples were excluded in a second analysis. This procedure intended to mitigate the effect of outliers, as the logarithmic measurement has a lot more impact in the overall statistical distribution of the results. Therefore, this analysis aims to provide a wider perspective of the results.

According to this analysis, the model that obtained the lowest value of MAE was the WinProp UDP Outdoor, with a value of 12.427 dB. The MAE of the WinProp UDP Indoor model also suffered a clear change. Initially it was 26.466 dB and it decreased to 13.712 dB. This result confirms that using the Outdoor version of the WinProp UDP is the best option to predict the signal level throughout the walk test route. The loss values associated to the building penetration and de-penetration used in Indoor version of the model are related to the structure and material of the buildings itself. However, in this analysis generic values of indoor losses were used instead. As shown in Figure 4.30, the indoor version of the WinProp UDP appears to have samples with a bigger difference to the walk test results than the outdoor version. Considering the majority of the received signal corresponds to the component that does not penetrate the buildings, the point-to-point results confirm a better correlation to WinProp UDP Outdoor than WinProp UDP Indoor. The fact that the entire walk test was conducted outdoors confirms once again the increased accuracy shown in the results of WinProp UDP Outdoor. Also, when comparing the point-to-point with the results obtained by area, it confirms the better fit of WinProp UDP Outdoor against its indoor version.

RSRP was also analysed according to the range level. The MAE and SD were calculated for two different RSRP intervals. In the first case samples of the walk test that had RSRP lower or equal to -85 dBm were analysed separately. This scenario attempts to interpret the results of the different models when the mobile terminal is located at a considerable distance from the base station. The model that obtained the lowest MAE in this case was COST 231-Hata. The second scenario only analyses walk test samples with a power level higher than -85 dBm. In this situation, when the receiver is located closer

to the base station the model that obtained the lowest MAE of all the different simulations was SPM 2D, which also registered the lowest standard deviation. This behaviour is once again surprising, specially given the low performance of this model in the entire range of measurements. In this sense, most of the error results from the mobile terminal being located in or close to the cell edge.

The surprisingly poor performance of SPM 2.5D is also noteworthy. The 2.5D database attributes an average loss value to each interval of clutter heights. If the range of heights attributed to each clutter class is too wide, the error associated tends to increase substantially. This model, although widely used internally, is calibrated to fit into a wide range of scenarios, with highly varied building heights, which is not the case of Antwerp city centre and that also helps to explain the relatively poor performance of SPM 2.5D compared with the remaining propagation models.

The model that overall seems to show a best performance regardless the method of analysis is WinProp UDP Outdoor. This model presents almost the best MAE when all samples are analysed together and a good match when splitting the RSRP into different categories, although for higher RSRP levels the MAE is slighlty degraded. In the area analysis section, WinProp UDP Outdoor is also the model that more consistently approximates to the results measured in the walk test. This behaviour can clearly be distinguished in the CDF plot of Figure 4.15 of the previous section. In the point-to-point comparison of the measured and simulated values, the outdoor version of WinProp UDP also proved its consistency.

When looking to RSRQ, it shows less variation than the RSRP. A possible cause for this is the fact the RSRQ measures the quality of the received reference signal over the RSSI, which is a measure of the entire bandwidth highly associated with other cells' interference. In this case both numerator and denominator are equally affected by the error. In the first analysis of the RSRQ results, the model that obtained the lowest error was WinProp UDP Outdoor with a MAE of 6.319 dB. It is worth noticing that both WinProp UDP simulations of the RSRQ results had more resolution constraints than the other models and obtained less valid points used in the calculation of the errors. The third analysis consisted in separating the walk test samples by intervals and analysing them separately. The walk test samples that had a RSRQ level lower than or equal to -8 dB were first analysed. In this case, the model that obtained the lowest MAE was WinProp UDP Outdoor. The model that obtained the lowest MAE in the scenario in which the receiver is located closer to the base station was WinProp UDP Indoor. It becomes clear that the conclusions reached in the analysis by coverage area are confirmed with the point-to-point RSRQ results.

Another important aspect is the fact that, incidentally, all base stations were located above rooftop level within the scenario under analysis. This is a typical scenario when a macro network requires capacity expansion and the proposed solution is to deploy small-cells. Under these conditions the traditional approach is to plan small-cells for coverage holes that the existing macro sites cannot cover or to improve network quality in locations where the existing macro network does not provide enough radio quality to allow higher order modulation schemes. However, it has not been possible to assess the behaviour of these propagation models applied to outdoor small-cells, traditionally deployed at street level at heights no higher than 2 floors and where most of the radio propagation happens below rooftop

level.

Regarding future work, it would be interesting to validate some of these results by recreating this study in other urban areas or even expand it to different scenarios and assess its validity. An equally valid experiment would be to recreate this exact study but changing the terminal and increasing the route so as to cover more clutter classes, across a wider area to better complement the measurement scenario and increase the amount of measured samples.

Bibliography

[1] S. Sesia, M. Baker, and I. Toufik. *LTE – The UMTS Long Term Evolution: From Theory to Practice*. John Wiley & Sons, Chichester, 2009.

[2] Cisco, "Cisco Visual Networking Index: Global Mobile Data Traffic Forecast Update, 2016-2021", White Paper, Cisco Systems, USA, February 2017. [Online] Available: `https://www.cisco.com/c/en/us/solutions/collateral/service-provider/visual-networking-index-vni/mobile-white-paper-c11-520862.pdf`, consulted on March 2018.

[3] H. Holma and A. Toskala. *LTE for UMTS-OFDMA and SC-FDMA based Radio Access*. John Wiley & Sons, Chichester, 2009.

[4] LTE tutorials: E-UTRAN Architecture. [Online] Available: `http://www.artizanetworks.com/resources/tutorials/eut_arc.html`, consulted on October 2017.

[5] Alcatel Lucent, "The LTE Network Architecture — A comprehensive tutorial". Strategic White Paper. 2009.

[6] H. Holma and A. Toskala. *WCDMA for UMTS: HSPA Evolution and LTE*. John Wiley & Sons, Chichester, 2007.

[7] E. Dahlman, S. Parkvall, J. Sköld, and P. Beming. *3G Evolution: HSPA and LTE for Mobile Broadband*. Academic Press, Oxford, 2007.

[8] [Online] Available: `https://www.anacom.pt/render.jsp?categoryId=383094`, consulted on October 2017.

[9] B. Hanta. "SC-FDMA and LTE Uplink Physical Layer Design". *Seminar LTE: Der Mobilfunk der Zukunft, University of Erlangen-Nuremberg, LMK*, 2009.

[10] Y. Zhou, Z. Lei, and S. H. Wong. "Evaluation of Mobility Performance in 3GPP Heterogeneous Networks". *Proc. IEEE 79th Vehicular Technology Conf.*, pages 1–5, May 2014.

[11] A. Ulvan, R. Bestak, and M. Ulvan. "The Study of Handover Procedure in LTE-based Femtocell Network". In *Wireless and Mobile Networking Conference (WMNC), 2010 Third Joint IFIP*, pages 1–6. IEEE, 2010.

[12] J. Zhang and G. De la Roche. *Femtocells: technologies and deployment*. John Wiley & Sons, Chichester, 2010.

[13] 3GPP. *TS 32.591: Telecommunication management; Home enhanced Node B (HeNB) Operations, Administration, Maintenance and Provisioning (OAM&P); Concepts and requirements for Type 1 interface HeNB to HeNB Management System (HeMS)*, .

[14] Cisco. *HeNB-GW Administration Guide, StarOS Release 21.2*. [Online] Available: `https://www.cisco.com/c/en/us/td/docs/wireless/asr_5000/21-2/HeNB-GW/21-2-HeNBGW-Admin/21-2-HeNBGW-Admin_chapter_01.pdf`, consulted on October 2017.

[15] 3GPP. *Heterogeneous Networks in LTE*, . [Online] Available: `http://www.3gpp.org/technologies/keywords-acronyms/1576-hetnet`, consulted on October 2017.

[16] M. Paolini. "Interference Management in LTE Network and Devices". White Paper, Senza Fili Consulting, USA, 2012, [Online] Available: `http://www.senzafiliconsulting.com/Resources/WhitePapers.aspx`, consulted on October 2017.

[17] M. S. Ali. "An Overview on Interference Management in 3GPP LTE-Advanced Heterogeneous Networks". *International Journal of Future Generation Communication and Networking*, 8(1):55–68, 2015.

[18] H.-W. Kwak, P.-U. Lee, Y.-H. Kim, N. Saxena, and J.-T. Shin. "Mobility Management Survey for Home-e-NB Based 3GPP LTE Systems". *Journal of Information Processing Systems*, 4(4):145–152, 2008.

[19] F. Letourneux, S. Guivarch, and Y. Lostanlen. "Propagation Models for Heterogeneous Networks". In *Proc. of 7th European Conference on Antennas and Propagation (EuCAP 2013)*, pages 3993–3997, Gothenburg, Sweden, 2013. IEEE.

[20] N. Nkordeh, A. Atayero, F. Idachaba, and O. Oni. "LTE Network Planning using the Hata-Okumura and the COST-231 Hata Pathloss Models". *Proceedings of the World Congress on Engineering*, I, 2014.

[21] R. Hoppe, P. Wertz, F. M. Landstorfer, and G. Wölfle. "Advanced Ray-Optical Wave Propagation Modelling for Urban and Indoor Scenarios Including Wideband Properties". *Transactions on Emerging Telecommunications Technologies*, 2003.

[22] S. Sousa, F. J. Velez, and J. M. Peha. "Impact of Propagation Model on Capacity in Small-Cell Networks". In *Performance Evaluation of Computer and Telecommunication Systems (SPECTS), 2017 International Symposium on*, pages 1–8. IEEE, 2017.

[23] A. O. Kaya and D. Calin. "Modeling Three Dimensional Channel Characteristics in Outdoor-to-Indoor LTE Small Cell Environments". In *Military Communications Conference, MILCOM 2013-2013 IEEE*, pages 933–938. IEEE, 2013.

[24] ”Performance Analysis of Empirical Propagation Model for Long Term Evolution (LTE) Network”, author=Milanović, Josip and Šimac, Gordan and Mazor, Krešimir, booktitle=Smart Systems and Technologies (SST), International Conference on, pages=69–74, year=2016, organization=IEEE.

[25] L. Song and J. Shen. *Evolved Cellular Network Planning and Optimization for UMTS and LTE*. CRC Press, 2010.

[26] A. F. Molisch. *Wireless Communications*, volume 34. John Wiley & Sons, 2011.

[27] R. Hoppe. ”An Introduction to the Urban Intelligent Ray Tracing (IRT) Prediction Model”. *AWE Communication GmbH*, September 2005.

[28] ”WinProp Plug-In User Reference Guide”. AWE Communication GmbH, February, 2012 [Online] Available: `http://alfin.dosen.st3telkom.ac.id/wp-content/uploads/sites/8/2015/12/AtollPlugIn.pdf`, consulted January 2018.

[29] R. Wahl, G. Wölfle, P. Wertz, P. Wildbolz, and F. Landstorfer. ”Dominant Path Prediction Model for Urban Scenarios”. *14th IST Mobile and Wireless Communications Summit, Dresden (Germany)*, 2005.

[30] G. Wolfle and F. M. Landstorfer. ”Dominant Paths for the Field Strength Prediction”. In *VTC ’98. 48th IEEE Vehicular Technology Conference. Pathway to Global Wireless Revolution (Cat. No.98CH36151)*, volume 1, pages 552–556, May 1998.

[31] Visicom. [Online] Available: `https://visicom.ua/products/data_for_wireless_planning?lang=en`, consulted on January 2018.

[32] M. Brau, Y. Corre, and Y. Lostanlen. “Assessment of 3D Network Coverage Performance from Dense Small-Cell LTE”. In *International Conference on Communications (ICC)*, pages 6820–6824. IEEE, 2012.

[33] T. Alwajeeh, P. Combeau, R. Vauzelle, and A. Bounceur. ”A High-Speed 2.5 D Ray-Tracing Propagation Model for Microcellular systems, application: Smart cities”. In *Antennas and Propagation (EUCAP), 2017 11th European Conference on*, pages 3515–3519. IEEE, 2017.

[34] A. Mukhopadhyay, H. Batteram, X. Chen, F. Louwdyk, A. Sharma, and J. Zhao. ”Designing Optimal Heterogeneous Networks”. In *Sarnoff Symposium, 2016 IEEE 37th*, pages 47–52. IEEE, 2016.

[35] E. Mellios, G. S. Hilton, and A. R. Nix. “Ray-Tracing Urban Picocell 3D Propagation Statistics for LTE Heterogeneous Networks”. In *7th European Conference on Antennas and Propagation (EuCAP)*, pages 4015–4019. IEEE, 2013.

[36] S. Hamim and M. Jamlos. “An Overview of Outdoor Propagation Prediction Models”. In *2nd International Symposium on Telecommunication Technologies (ISTT)*, pages 385–388. IEEE, 2014.

[37] R. Wahl and G. Wölfle. ”Combined Urban and Indoor Network Planning Using the Dominant Path Propagation Model”. *1st European Conference on Antennas and Propagation (EuCAP 2006)*, pages 1–6, 2006.

[38] S. I. Popoola and O. F. Oseni. ”Performance Evaluation of Radio Propagation Models on GSM Network in Urban Area of Lagos, Nigeria”. *International Journal of Scientific & Engineering Research*, 5(6):1212–1217, 2014.

[39] P. Sabatier. 9955 Default Propagation Models Recommended for 400MHz up to 5.5GHz. Nokia Internal Document.